SC71096.FR

Micro-Optic Color Separation Technology for Efficient Projection Displays

Final Report

Contract No. NAS2-14041

Prepared for:

Contracting Officer's Rep.
J. Larimer - M/S 269-6
NASA/Ames Research Center
P.O. Box 1000
Moffett Field, CA 94035-1000

Prepared by:

W.J. Gunning and E. Boehmer
Rockwell Science Center
1049 Camino Dos Rios
Thousand Oaks, CA 91360

March 1997

Rockwell

Science Center

Copy # 8

REPORT DOCUMENTATION PAGE

Form Approved
OMB No. 0704-0188

1. AGENCY USE ONLY *(Leave Blank)*	2. REPORT DATE	3. REPORT TYPE AND DATES COVERED
	March 1997	Final Report 05/09/94-08/09/95

4. TITLE AND SUBTITLE
Micro Optic Color Separation Technology

5. FUNDING NUMBERS
NAS2-14041

6. AUTHOR(S)
W.J. Gunning and E. Boehmer

7. PERFORMING ORGANIZATION NAME(S) AND ADDRESS(ES)
Rockwell Science Center, Inc.
P.O. Box 1085
Thousand Oaks, CA 91358

8. PERFORMING ORGANIZATION REPORT NUMBER
SC71096.FR

9. SPONSORING / MONITORING AGENCY NAME(S) AND ADDRESS(ES)
NASA/Ames Research Center
P.O. Box 1000
Moffett Field, CA 94035-1000
ATTN: Contracting Officer
Technical Rep. J. Larimer
M/S 269-6

10. SPONSORING / MONITORING AGENCY REPORT NUMBER

11. SUPPLEMENTARY NOTES

12a. DISTRIBUTING/AVAILABILITY STATEMENT

12b. DISTRIBUTION CODE

13. ABSTRACT *(Maximum 200 Words)*

Phase I of this project focused on development of an overall optical concept which incorporated a single liquid crystal spatial light modulator. The system achieved full color by utilizing an echelon grating, which diffracted the incident light into three orders with different color spectra, in combination with a microlens array, which spatially separated RGB bands and directed the light of the appropriate wavelength to the appropriate color dot. Preliminary echelon grating designs were provided by MIT/LL and reviewed by Rockwell. Additional Rockwell activities included the identification of microlens designs, light sources (ILC), and projection optics to fulfill the overall design requirements. An internal subcontract was established with Rockwell's Collins Avionics and Communications Division (CACD) which specified the liquid crystal SLM (Sharp Model No. LQ 46E02) and built the projection display baseline projector. Full Color projected video images were produced and shown at the '95 HDS meeting in Washington. Analysis of the luminance performance of the projector and detailed parameter trade studies helped define the dependence of overall display efficiency on lamp collimation, and indicated that a lamp with very small arc dimension is required for the optical concept to be viable.

14. SUBJECT TERMS
Projection displays, light value, refractive microlenses, micro-optics, echelon grating, ion etching, short arc,

15. NUMBER OF PAGES
54

16. PRICE CODE

17. SECURITY CLASSIFICATION OF REPORT	18. SECURITY CLASSIFICATION OF THIS PAGE	19. SECURITY CLASSIFICATION OF ABSTRACT	20. LIMITATION OF ABSTRACT
UNCLASSIFIED	UNCLASSIFIED	UNCLASSIFIED	UL

TABLE OF CONTENTS

List of Figures

1. Summary

1.1. Technical Background

Liquid crystal display devices have not been able to replace cathode ray tubes (CRTs) for projection purposes since their low optical throughput and higher cost more than outweigh their advantage of power efficiency. The low display transmission is the result of cumulative losses from many optical elements. A schematic drawing of liquid crystal light valve (LCLV) assembly is shown in *Fig. 1*. The input polarizer causes an immediate loss of 50% and further, typical peak transmissions of the transmitted polarization are ~ 80% per element. An additional loss factor is the aperture ratio of the liquid crystal display panel (ratio of clear area to obscured area) which may be less than 50% for high resolution panels. For full color displays the transmission is further limited by the absorptive color filter array, since each color dot only transmits within its designated color band, the other two colors are being absorbed. Assuming *ideal* color filters, the total transmittance is reduced by a factor of three. Thus, typical AMLCD transmittance is roughly 5.3%, neglecting light losses due to a diffuser which would be required for a direct view backlit display. The absorption losses that are present in a projection display impose additional restrictions, namely on lamp power, lamp life, display cooling or a tradeoff between lamp power and brightness.

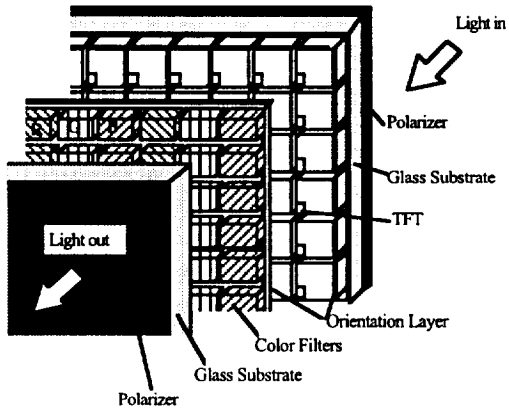

Fig. 1 Schematic view of an active matrix liquid crystal light valve.

If AMLCDs are to replace CRTs for projection purposes optical concepts which are significantly improved with respect to brightness or power must be developed. These improvements can be achieved if:

- Optical means can be used to direct light of specific colors to the appropriate color dot, yielding a factor of three increase in throughput.
- Color separation can be made sufficiently precise, such that color filter requirements can be relaxed, or color filter arrays can be eliminated entirely.
- Eliminating the filter array could have additional cost benefits as the color filter array represents a significant cost element for the display panel.

A number of liquid crystal projection display configurations have been proposed or developed.[1] The baseline concept against which all other approaches will be compared features a single full color LCLV which is directly illuminated by the lamp, see *Fig. 2*. This is the most compact and cost effective optical projection architecture, however, the system has poor luminous efficiency due to color filter losses and low resolution.

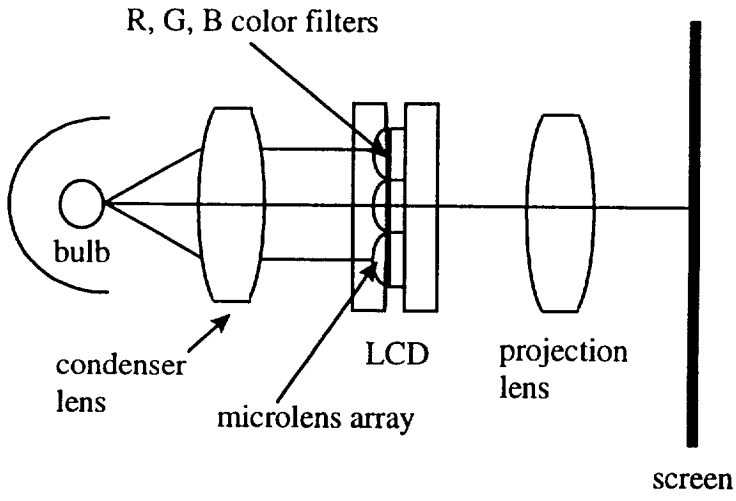

Fig. 2 A single light valve projector is the most compact and cost-effective optical projection architecture, however, there is poor luminous efficiency due to color filter losses and low resolution.

The most common approach utilizes three monochrome LCLVs. A schematic drawing of the optical train is shown in *Fig. 3*. Each display projects a scene for a single color band (red, green, blue). Thus, each LCLV operates as a monochrome panel and the 67% loss due to a color filter array is avoided. Full color is achieved by passing these three scenes through a dichroic beam combiner. This concept achieves higher scene resolution with higher optical efficiency and fused color, however, at the expense of increased weight, volume and cost. Having three LCLVs rather than one adds complexity, losses at dichroic combiners and requires precise optical alignment.

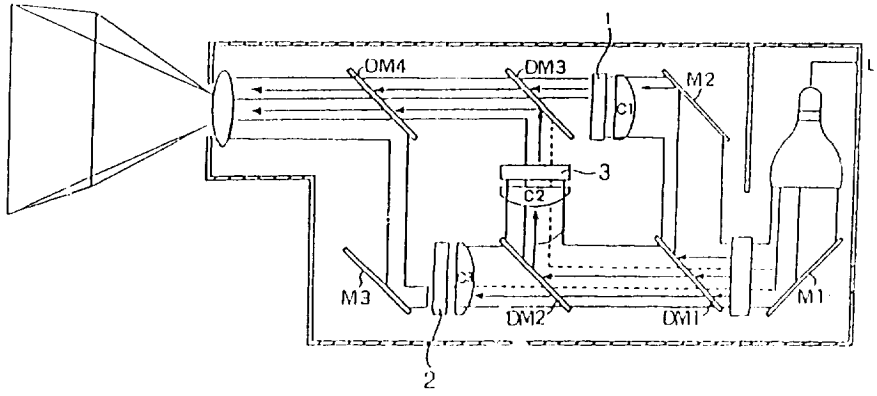

Fig. 3 Optical train for a projection display configuration using three monochrome LCLVs, a higher scene resolution approach with higher optical efficiency and fused color at the expense of weight, volume and cost. 1-3 = LCVS, M1-M3 = turning mirrors, C1-C3 = collection lenses, DM1-DM3 = dichroic mirrors, L = light source.

Another design attempts to recover optical losses resulting from the insertion loss of optical elements by using three single color LCLVs and two dichroic mirrors.[2] The illuminating beam is divided according to polarization and each beam is reflected from a separate display as schematically displayed in *Fig. 4*. The resulting images are then combined. This approach trades marginal improvement in efficiency against added cost, weight and increased requirements for optical alignment.

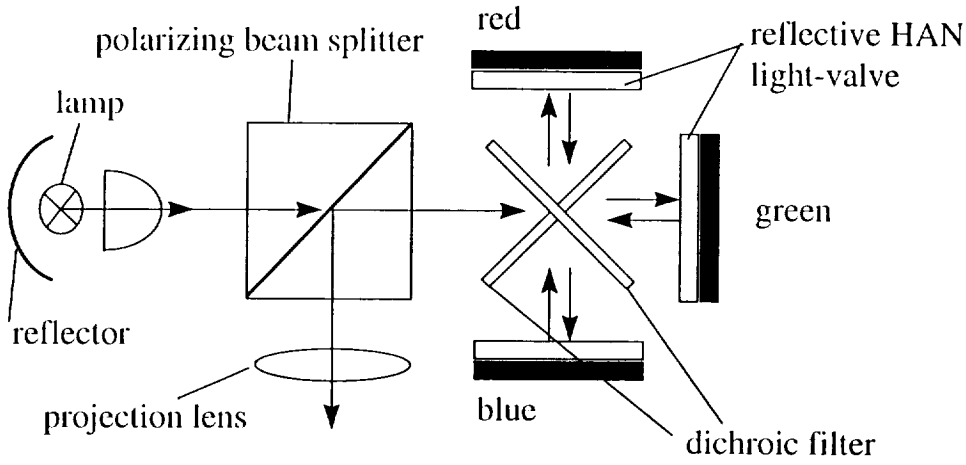

Fig. 4 Reflective LCLV approach trades marginal improvement in efficiency against added cost, weight and increased requirements for optical alignment.

Sharp Corp. has a concept based on a single LCLV which achieves higher efficiency by directing each of the 3 color bands to the appropriate color dot, overcoming the 66% color filter array losses. This is accomplished by separating the R, G, B color bands via reflection from a series of thin film dichroic mirrors (U.S. patent No. 5,161,042), *see Fig. 5*. Each mirror generates a spectrally tailored beam that impinges on the display at a specific angle of incidence. A separate microlens array collects and redirects the light to the appropriate color dot. This approach requires a folded optical path and therefore does not result in the most compact design. Further, the dichroic thin film mirrors are expensive and require precise alignment.

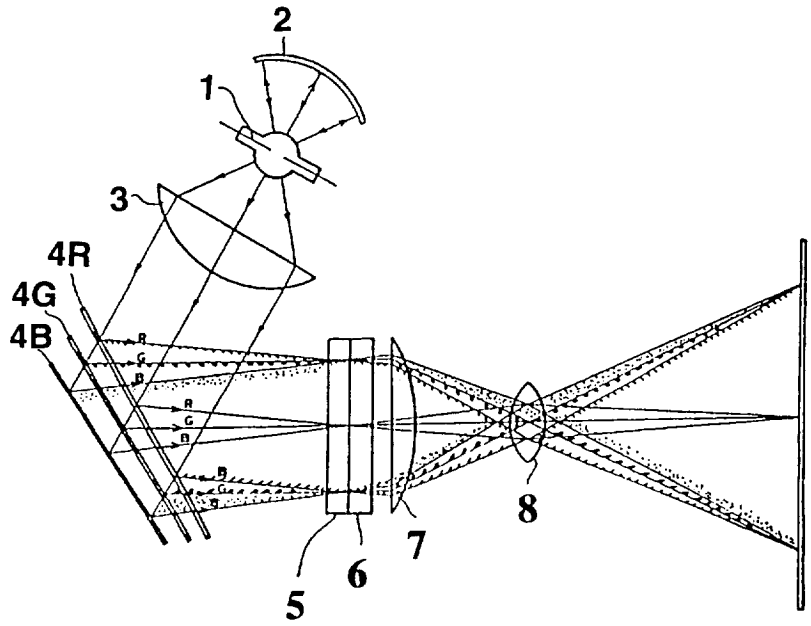

Fig. 5 Single light valve color separation concept using dichroic mirrors, Sharp Corp. U.S. patent No. 5,161,042. This approach offers little volume reduction and requires additional optical elements, and careful alignment. 1 = light source, 2,3 = light source collection and collimation optics, 4R,4G,4B = dichroic mirrors for color separation, 5 = microlens array, 6 LCLV, 7,8 = projection optics.

The projection display concept developed under this program focuses on increasing the optical efficiency of a single light valve color projection system via a micro-optics based color separation technique which utilizes all the light emitted by an illumination source at all times. It exploits the unique ability of an echelon grating structure to separate an incident beam into three, angularly separate, distinct spectrally bands. A schematic view of the beam train is presented in *Fig. 6.* Projector compactness and simplicity with respect to alignment are increased since transmissive rather than reflective (or folded, see Sharp dichroic approach) optics are used. Efficient color separation by diffraction with micro-optical components into distinct spectral orders avoids expensive thin film dichroics and may eliminate the need for color filters entirely. Microlenses registered to color groups rather than single pixels are used to direct the RGB bands to the appropriate pixel and to overcome the LCLV clear aperture ratio.

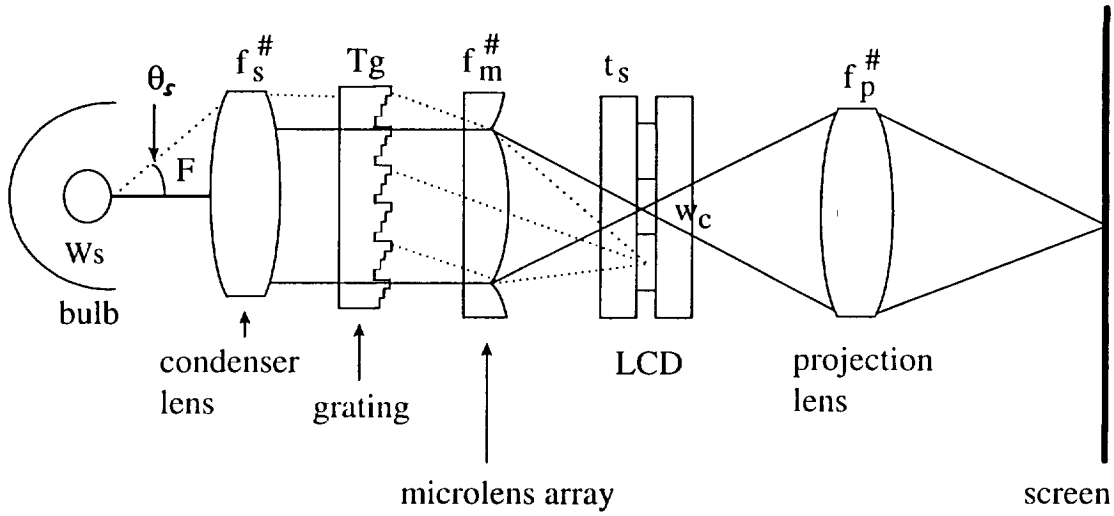

Fig. 6 Optical beam train of the Rockwell / MIT/LL single light valve color projection system based on color separation via micro-optics offers greater brightness, optical simplicity and reduced cost at no expense of resolution as compared with competitive single LCLV projectors. θ_S = maximum full angular beam spread of illumination source, w_S = arc length, F = condenser lens focal length, $f_S\#$ = condenser lens f/number, T_g = grating period, $f_m\#$ = microlens f/number, t_S = display glass substrate thickness, w_c = color dot pitch, $f_p\#$ = projection lens f/number.

The micro-optics based color separation single light valve concept is potentially cheaper and has less weight and volume than concepts which utilize three or two separate light valves, however, at the expense of reduced resolution. This approach also requires a well collimated source in order to avoid color cross talk and to enable a micro-optic grating design having the best efficiency. Compared to a single LCLV projector, our design offers greater brightness, optical simplicity and reduced cost since micro-optical components may be inexpensively replicated in plastic.

1.2. *Program Summary*

The object of this work was to improve the optical efficiency of projection liquid crystal displays for large area presentation requirements. Methods were to be employed which reduce cost, size and power requirements and low cost manufacturing methods were to be developed for optical components. Micro-optic components were to be integrated into existing projection

displays with minor modification. Achieving these goals required the following actions during Phase I:

(i) Joint development of an overall optical design between Rockwell and MIT/LL based on an echelon grating / microlens array for pixel-by-pixel color separation, end-to-end analysis of required optical projector components and trade space development to specify micro-optical components that are compatible with available LCLV panel specifications. MIT/LL had overall responsibility for echelon grating fabrication and low cost replication techniques.

(ii) Process development for micro-optics manufacturing according to baseline projector design and optical component specifications, prototype micro-optics fabrication, characterization and demonstration of color separation concept.

(iii) Integration of micro-optical components into a baseline projector in collaboration with Collins Avionics and Communication Division (CACD) to establish practical performance limits and assess methods for further display performance optimization, component replication methods and potential commercial applications.

During the first Phase of this project (reported here) an overall optical concept was developed which incorporated a single liquid crystal spatial light modulator. The system achieved full color by utilizing an echelon grating, which diffracts incident light into three orders with different color spectra, in combination with a micro-lens array, which spatially separates the RGB bands and directs light of the appropriate wavelength to the appropriate color dot. Preliminary echelon grating designs were provided by MIT/LL and reviewed by Rockwell. Additional Rockwell activities included the identification of microlens designs, light sources (ILC, Sharp) and projection optics to fulfill the overall design requirements. An internal subcontract

was established with Rockwell's Collins Avionics and Communications Division (CACD) which specified the liquid crystal light valve (Sharp Model No. LQ 46E02) and built the baseline display projector. Performance goals for the prototype projector compared to the Sharp baseline model are presented in Table 1. Full color projected video images were produced and demonstrated at the '95 DARPA High Definition Systems Information Exchange Conference. Analysis of the luminance performance of the projector and detailed parameter trade studies helped to define the dependence of overall display efficiency on lamp collimation and indicated that a lamp with very small arc dimension is required for this concept to be viable.

2. Color Separation Optics for LCD Projection Systems

The key feature of the Rockwell / MIT/LL projector design is a grating that separates colors by order rather than by dispersion within each order. The potential of such gratings for commercial applications was discussed by Dammann.[3] Echelon (stair step) gratings have optical properties which give them a significant advantage over conventional blazed gratings when used for color separation in liquid crystal projection systems. Compared to a blazed grating, the angular wavelength separation achievable with an echelon grating is significantly larger and there is less of an angular offset of the spectrally dispersed beam. In addition, the grating period that is required to produce a given angular separation is large, which reduces fabrication complexity.

In *Fig. 7,* the differences between a conventional dispersion (blazed) grating and an echelon grating are highlighted. The efficiency curves clearly show that the blazed grating has its greatest efficiency for all wavelengths in a single order while the echelon grating can be tuned to produce higher spectrally selective diffraction efficiency into adjacent orders. In our design the height of each step of the echelon grating is equal to one wave optical path for the green wavelength, thus the green light is undeviated in zero order. The blue has its maximum diffraction efficiency in the plus one order and the red in the minus one order. Such a grating having four steps and a 16 micron period was fabricated by Farn et al. at Lincoln Laboratories.[4] The performance of this

grating when combined with a microlens array proved that it could indeed facilitate efficient color separation in liquid crystal color display projection systems. The overall design of an actual full color single light valve projector incorporating an echelon grating and a microlens array is shown in Fig. 8. Basic design considerations will be discussed below.

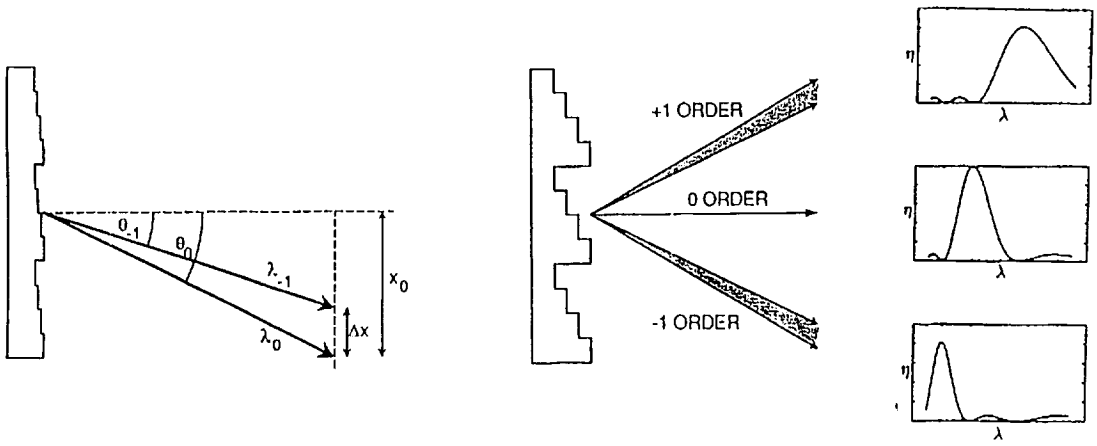

Fig. 7 Comparison between dispersion (blazed) and diffraction (echelon) grating. The blazed grating has its greatest efficiency for all wavelengths within a single order while the echelon can be tuned to produce higher spectrally selective diffraction efficiency into adjacent orders.

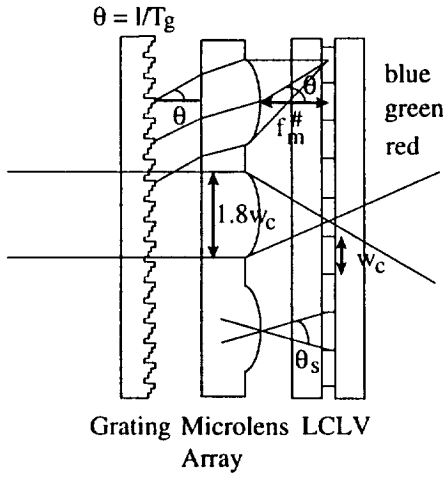

Fig. 8 Echelon microlens liquid crystal color separation scheme. θ = etchelon grating diffraction angle, w_c = color dot pitch, θ_s = maximum full angular beam spread for the illumination source, $f_m^{\#}$ = microlens f/number.

2.1. Basic Projector Design Considerations

The design of a prototype projector with micro-optics color separation required careful review of constraints imposed by available micro-optics production techniques and commercially obtainable components as well as careful modeling of the highly interactive component properties of the optical train. One of the fundamental design constraints was the restriction of the display pixel layout to a block wall (color triad) pattern. In the ideal implementation the microlenses are rectangular, exactly covering a complete R, G, B color pixel. These lenses can be made with binary optics to achieve fill factors of 100%. However, binary optic microlenses are strongly dispersive and cannot maintain high efficiency over the complete range of visible wavelengths. Further, binary optic lenses of the necessary size are limited to f/7.6, because at that speed the smallest producible feature size on the lens is 1 μm. This f/# limitation makes the approach unsuitable for this application. Refractive microlenses only exhibit normal chromatic dispersion and can achieve much lower f/numbers than binary optic lenses of similar size, but with current techniques they can only be made round. The current restriction to round lenslets in the overall optical design required each lenslet to be centered on an RGB color group. Arrangements having stripe filters lead to reduced fill factor. A staggered array of round lenslets used in a block wall pattern can achieve a maximum optical fill factor of 85%. Microlens array and color pixel layouts are illustrated in *Fig. 9*. These arrangements also require a black matrix film between the microlenses. It is also clear from this discussion that RGBG and RGBW pixel arrangements cannot be accommodated with our approach.

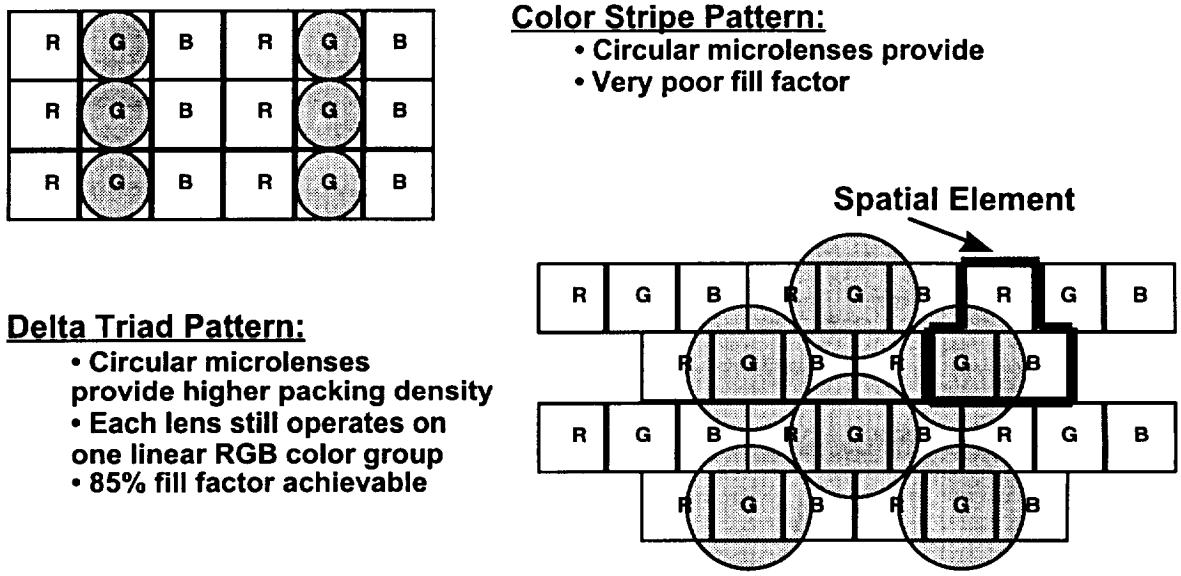

Fig. 9 Staggered array of round microlenses used in a block wall pattern have a maximum optical fill factor of 85%.

It is clear that an array of rectangular (or square) microlenses could increase efficiency and eliminate the need for a black matrix layer. Rockwell is continuing to develop fabrication methods to realize higher fill factor refractive microlenses for this and other applications.

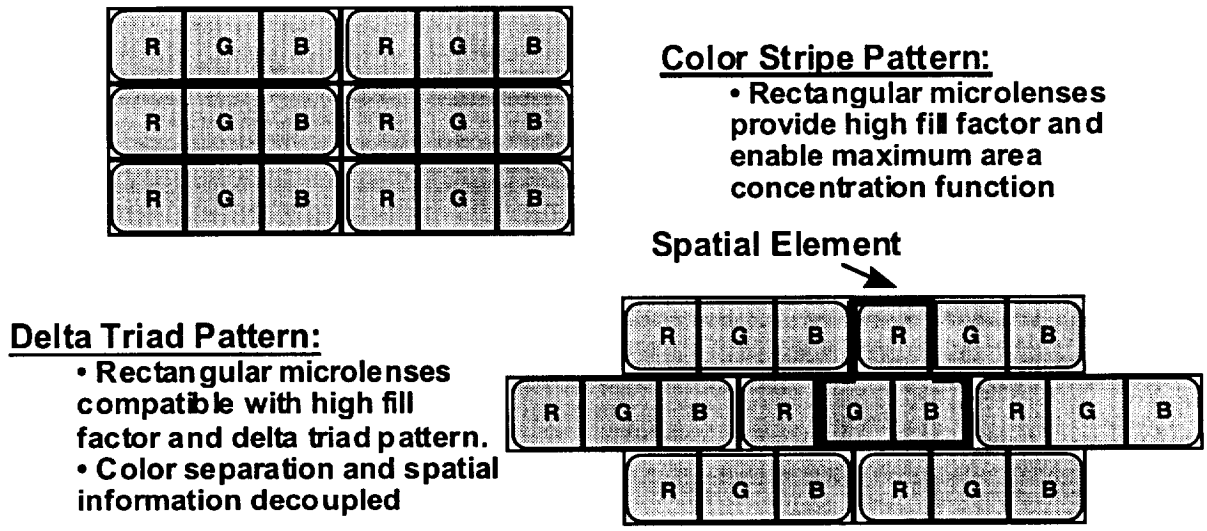

Fig. 10 Rectangular microlenses allow for an optimum fill factor of ~ 100%.

The choice of the liquid crystal light valve influences design parameters of the entire optical train of the projector. Interactions between individual optical components can best be elucidated by following the optical train from the LCD back to the illumination system. The interdependence between LCD and microlens properties can be deduced from *Fig. 9*. It is clear from this arrangement that the lenslet diameter is a function of pixel width. The centers of two lenslets must be offset by a full pixel width down and 1.5 pixel widths horizontally which results in a lenslet diameter of 1.8 pixel widths. Constraints on the focal length of the microlens array follow from *Fig. 8*, which shows that the focal point of the microlens array should be positioned at the plane of the liquid crystal. Therefore, the minimum focal length will be determined by the thickness of the LCLV substrate and polarizer. The substrate thickness on the screen side of the LCD is not restricted and may be varied if needed.

Properties of the LCLV panel and echelon grating are also strongly coupled. The echelon grating defracts the collimated light from the illumination system angularly into R, G, B bands. *Figure 8* shows the angular separation provided by the grating must be sufficient for the microlenses to direct and focus the colored beams into appropriate color pixels. The red and blue beams of light pass through the microlens array at the diffraction angle imposed by the grating and will have to come to focus one pixel width above or below the optical axis of the lenslet in order to avoid color spill-over by overlapping color bands. It is clear from this requirement that the focal point of the microlens array and grating diffraction angle are a function of pixel width and substrate thickness. Angular separation provided by the grating, i.e. the grating diffraction angle, is governed by the grating period as the most important grating design parameter.

Another design requirement is that an illumination system with high brightness, high collimation efficiency and commercially attractive dimensions and power consumption requires a light source resembling a point. As shown in *Fig. 11,* the full angular beam spread of a real source is given by the length of the arc or width of the bright part of the source and

the effective focal length of the collimation system. It is evident from *Fig. 6* that the chief ray from the bottom of the source through the center of the condenser lens can come to focus no higher than half a pixel width to avoid color cross talk. If the arc image height is restricted to half a pixel width, the grating imposed angular divergence is also reduced to half a pixel width. From these considerations, it follows that the total angular divergence of the illumination system must not exceed the diffraction angle of the grating.

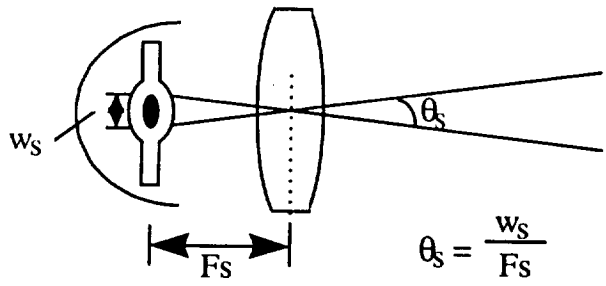

Fig. 11 Schematic drawing of an arc source, reflector and condenser lens. w_S = arc length, F_S = collection lens focal length, θ_S = maximum full angular beam spread for the illumination source.

Based on the general considerations given above, Rockwell Collins identified the Sharp display module Model No. LQ46E02 as the LCLV element best suited to the immediate requirements. This amorphous silicon LCLV was specifically designed for projector applications and was available in both monochrome and color versions with a 114 μm color dot pitch. Mechanical specifications of the display are given in Table 2, found in Section 6.

2.2. *Design Equations*

Section 2.1 elucidated the closely coupled nature of the optical system. In this section relationships are given and a model is described that predicts performance of the color separation device. Parameters include source size (typically a metal halide arc), grating period, number of grating steps, microlens focal length, color pixel cell width, and finally the

projector lens f/number. Effects of aperture ratios, color dispersion within each grating order and rigorous vector theory diffraction efficiencies are also considered.

Color separation is achieved by directing collimated white light onto the echelon grating, followed by a microlens array that focuses each color onto a separate color cell of LCLV. A schematic view of the optical train can be seen in *Fig. 6*. The green light, which is not diffracted, is focused on the cell positioned on-axis to the microlens. Other wavelengths are diffracted into an angle given by the grating equation

$$\theta = m\lambda/T_g \qquad (1)$$

where T_g is the grating period and m is the grating order (plus or minus one). These angles are those of the chief ray for the blue and red light entering the microlens. The chief ray is undeviated by the microlens and the beam comes to focus at the center of the adjacent color pixel in the LCLV. The diffraction angle can thus be expressed by

$$\theta = w_c/F$$

where w_c is the color dot center-to-center width, or pitch, and F is the microlens focal length. The following equation expresses the relationship between grating, microlens and color cell pitch.

$$T_g = \lambda F/ w_c \qquad (2)$$

It has to be taken into account that an actual illumination source is not a point but has a finite width, i.e. a finite arc length. The images formed by the microlens in each of the three colors demagnified images of the arc. The size of the arc's image at the LCLV, denoted by s, is given by,

$$s = w_s F/F_s \qquad (3)$$

where w_s is the size of the arc and F_s is an equivalent focal length of the collimation optics. The collimation lens and microlens in effect form an afocal telescope which demagnifies the source by the ratio of the focal lengths of the two lenses. To avoid losses due to the aperture mask at the LCD, it is required that the source image be smaller than the clear aperture. Thus,

$$s = w_s F/F_s < \sqrt{[A_r]}\, w_c \qquad (4)$$

where A_r is the aperture ratio of the LCD display. Combining equations (2) and (4) yields a constraint equation for the grating period.

$$T_g < s = \lambda F_s \sqrt{[A_r]}/w_s \qquad (5)$$

The right hand of equation (5) is the maximum value of the grating period necessary to avoid loss of light at the mask of the display. The maximum grating period, calculated as a function of arc lengths for different aperture ratios, is presented in *Fig. 12*. It was assumed that λ and F_s were 0.54 and 32.5 mm, respectively. These values were experimentally determined for a commercially available Sharp projector which was used to demonstrate the color separation concept. Specifications for the Sharp XV-P10U projector can be found in Table 3.

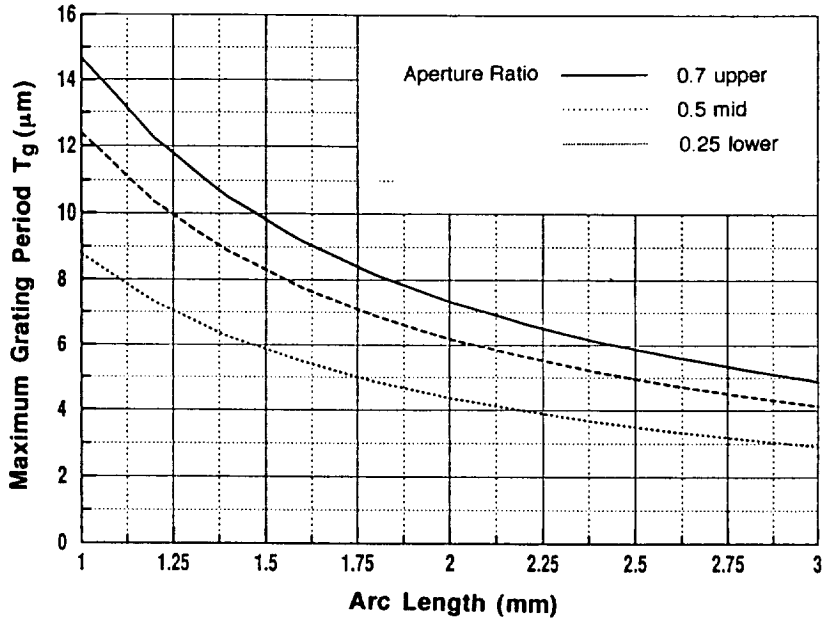

Fig. 12 Maximum grating period versus lamp arc size and various aperture ratios. Fixed collimating optics are assumed with an equivalent focal length of 32.5 mm. Results are plotted independent of cell color pitch.

Figure 12 shows the fundamental design curves for echelon grating color separation systems. For example, using a 3 mm arc length and 50% aperture ratio LCD light valve, the maximum usable grating period is 4 μm. For a 2 mm long arc, on the other hand, a grating period of 6 μm can be used, and for 1 mm arc length, the grating period increases to 12 μm. This result will be related to grating efficiency in section 2.3.

It is of interest to note that the color cell pitch cancels when equation (5) is formed from equations (2) and (4), which means that the results depicted in *Fig. 12* are independent of cell size, but do depend on aperture ratio. The constraint that limits equation (5) is that the focal length of the microlens in glass must exceed the source side substrate thickness of the LCD cell

$$n F > t_s \tag{6}$$

where n is the refractive index of the LCD substrate and t_s is its thickness. This leads to:

$$w_c T_g n / \lambda > t_s \tag{7}$$

The right hand side of equation (7) is the minimum substrate thickness. This quantity was plotted as a function of color cell width for various grating periods assuming $\lambda = 0.54$ μm and $n = 1.52$, as shown in *Fig. 13*. Standard substrate thicknesses for small LCLVs are now in the range of 0.5 – 1.1 mm.

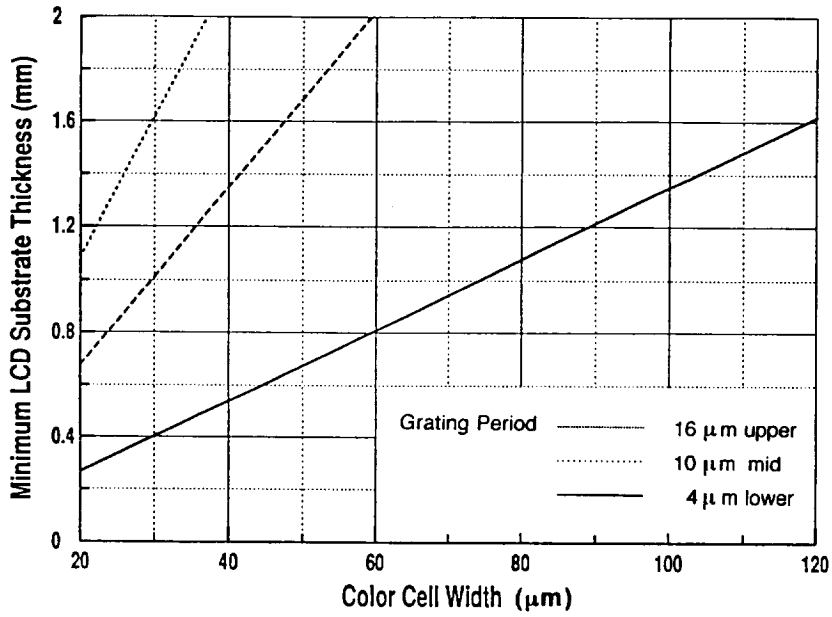

Fig. 13 Minimum LCLV substrate thickness versus color cell pitch for different grating periods. Gratings with periods greater than 10 μm are compatible with commercial substrate thicknesses of 1 – 1.6 mm.

Figure 12 can be used to determine the required grating period for any particular system. For example, for a source with an arc length of 3 mm and an aperture ratio of 50%, a 4 μm grating period is required. In order to find the minimum cell pitch for an LCLV with a 1 mm substrate thickness, the curve for the 4 μm grating in *Fig. 13* is found and its crossing point with the 1 mm substrate thickness line. The crossing occurs at a cell pitch value of ~ 75 μm. Smaller cell widths are not compatible with the arc length chosen for this example. It is clear from *Fig. 12*, however, what can be achieved with arc lengths of 1 - 2 mm. Grating periods of up to 14 μm may be used, which according to *Fig. 13* have no restraints with respect to substrate thickness. Gratings with a longer grating period are easier to produce and, as discussed later, have a higher diffraction efficiency. The relationship between grating period, grating efficiency and the effect on the overall system efficiency is described in the following section.

2.3. System Efficiency and Case Studies

Scalar diffraction theory predicts, exclusive of reflection losses, 100% diffraction efficiency for green and 91% for the red and blue contributions independent of the echelon grating period. However, scalar theory breaks down as the lateral dimensions of the grating become comparable to the wavelength as well as when the grating depth increases. *Figure 14* shows echelon grating diffraction efficiency as calculated at MIT/LL using rigorous coupled wave analysis[5] (short period 6-step gratings). It is suspected that scalar theory holds for 16 μm periods, but this was not verified. The values in the plot at 16 μm period are those taken from measurements of a four-step grating made at MIT/LL.

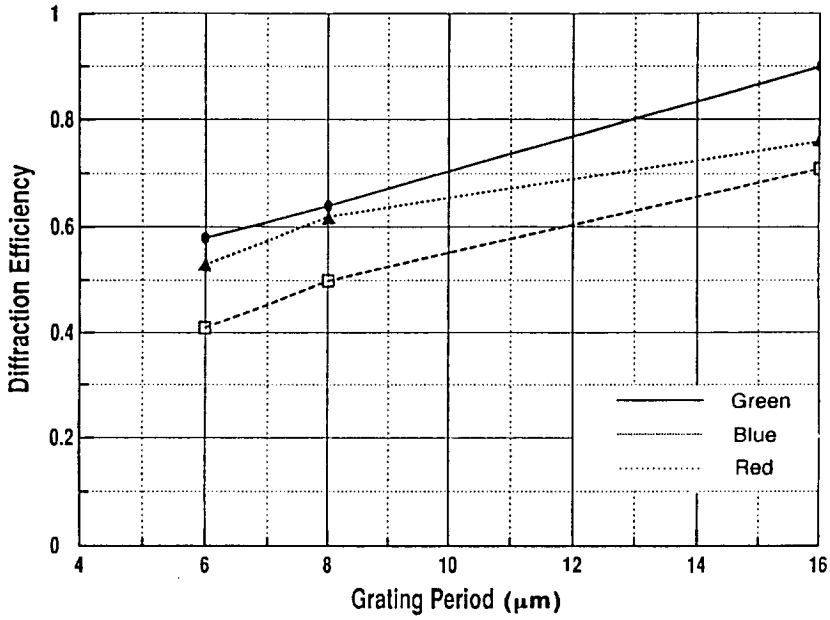

Fig. 14 Efficiency as a function of grating period for an echelon grating. The points at 6 and 8 μm period were calculated using rigorous coupled wave analysis for a six-step grating. The values at 16 μm were measured for a four-step grating made at MIT/LL.

A computer model was generated that predicts the end-to-end performance of the color separation system. The input parameters were arc length, grating period and number of steps, color cell width (pitch), and aperture ratio of the LCVC. Peak grating diffraction efficiencies,

for each of the three colors, were also included, as well as the effective focal length of the source collimator. The source was assumed to have unit intensity and to be uniform over all wavelengths. The model included the effect that the red diffracted order has a larger diffraction angle than blue which results in red light being focused further from the green and the blue light focused closer to the green. If the source image just fills the clear aperture for the green, then the red and blue will be clipped. The model assumes the green beam to be aligned on the microlens axis and does not show any enhancement to the red and blue which may be obtained by translating the microlens optical axis with respect to the green cell. The output is a data file giving the spectral content of each of the color cells. A listing of the computer code written in Power Basic is given in Appendix A.

The first system modeled had a cell pitch of 144 μm and a clear aperture ratio of 50%. The illumination source had an arc length a 3 mm. The grating had a grating period of 4 μm with four steps. The microlens was f/4.115 with a diameter of 205.2 μm (1.8 w_c). Design equations for the LCLV selected are given in Table 4. With the given constraints the LCLV substrate thickness may be up to 1.28 mm thick. The calculated spectral content for the green, blue and red color cells for the color separation system is presented in *Fig. 15*. The green cell rises to an intensity of 0.6, which is a consequence of the low grating diffraction efficiency (60% for green). Diffraction efficiencies for blue and red were even lower, 59% and 42%, respectively. Since the model is designed not to overfill the green cell, the red and blue bands experience some clipping. For comparison, a conventional single pixel design utilizing perfect color filters and perfectly efficient microlenses on each color dot would yield three curves with each peak rising to only 0.3 on the plot. The color rendition of these filters, however, would be consistent with standard bandpass filter transmission curves that are optimized for human eye response, as shown in *Fig. 16*. The R, G, and B bands rendered by the echelon grating deviate from standard filter curves especially in the red, which is shifted to longer wavelengths. This is a direct result of the short period 4-step echelon grating design

imposed by arc length and LCD panel design. An increase of the number of grating steps to six decreases the free spectral range and increases the resolving power of the grating. The red and blue bands would thus be shifted to overlap with standard color filter bands. The feature size of such a grating, however, would be beyond what can be processed with current production methods. Consequently, gratings with larger periods were explored.

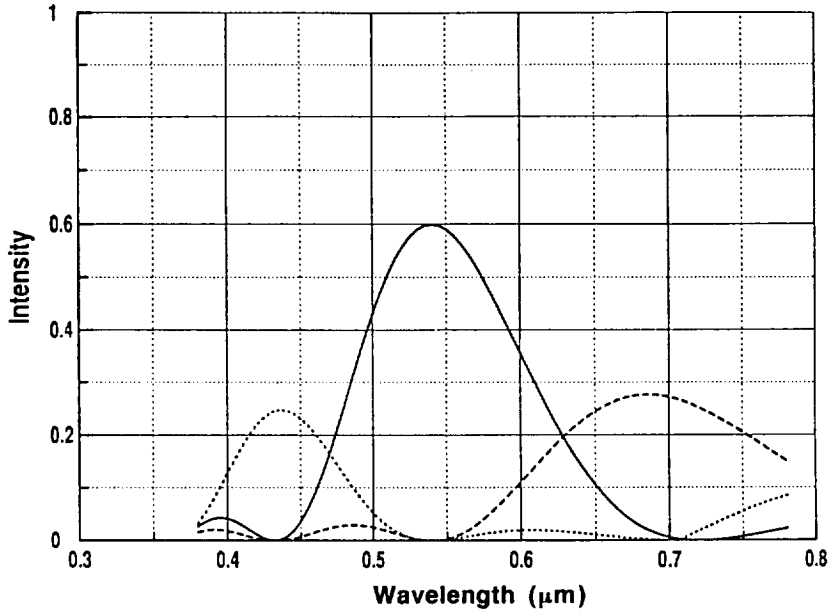

Fig. 15 Color band intensity for each color cell using the grating color separation for a system consisting of an arc of 3 mm, a 4 μm four step grating, 50% aperture ratio, and cell pitch of 114 μm. A rough comparison with filters only would yield a green intensity maximum at 0.33.

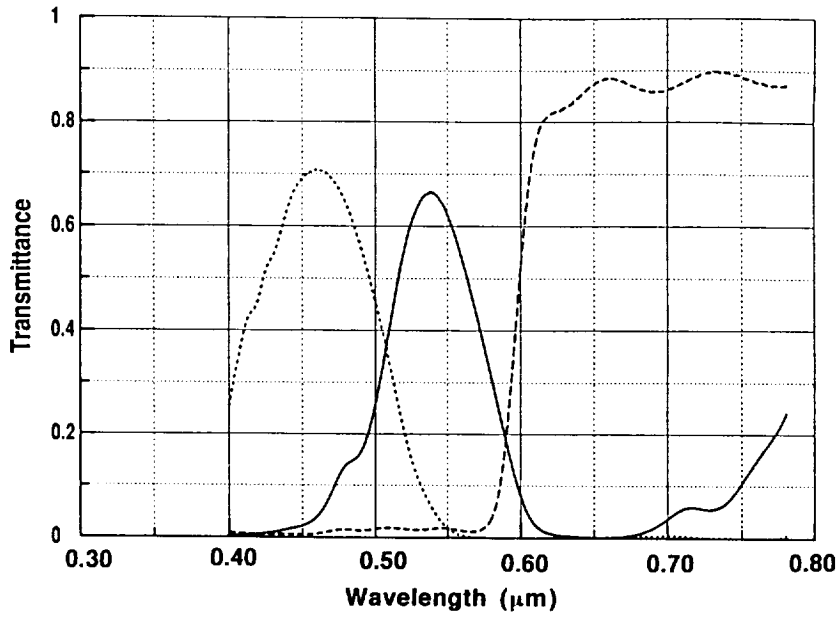

Fig. 16 Sharp standard color filter transmission curves.

The next color separation system was *identical* to the one given above with the exception of an aperture ratio of 27%, which more accurately reflects the design of the Sharp LCLV. The resulting spectral intensities, shown in *Fig. 17,* are clearly much lower compared to the previous case because of blocking experienced by all three colors. Efficiency is limited by the very

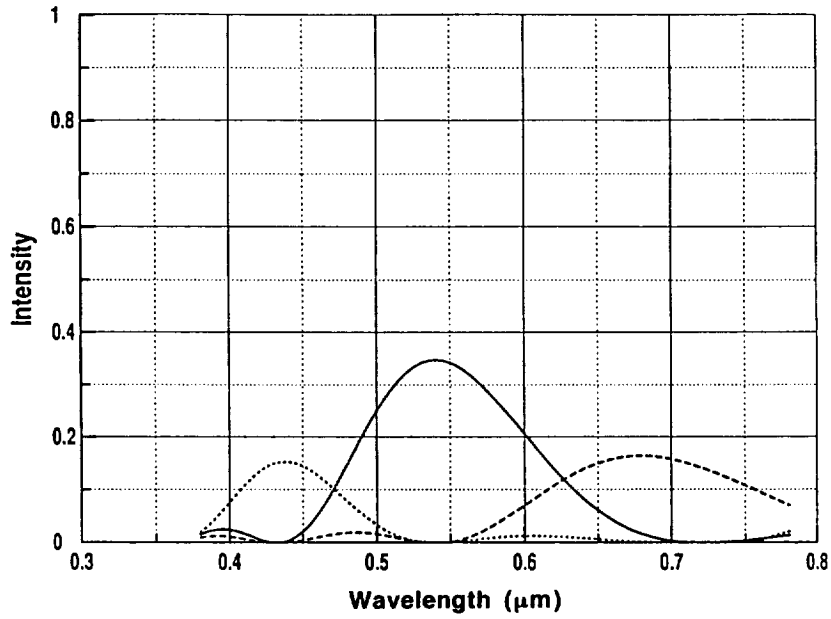

Fig. 17 Same conditions as in Fig. 6. For an accurate comparison, the microlens array in the Sharp design resulted in an effective aperture ratio of only 27%, far below the desired 100%.

The final case study was a system with a 30 μm pitch and an aperture ratio of 70%, representative of projection using a high resolution, polysilicon LCLV. The illumination source was assumed to have a 1 mm long arc. Availability of short arc sources is discussed in section 3.1. Using *Fig. 12,* a 6-step, 14 μm grating was selected. The microlens array was f/14.4, and the maximum LCLV substrate thickness could be as great as 1.182 mm. Results are given in *Fig. 18.* It is apparent that not only the system efficiency increased, but that in addition the color band maxima moved closer together and the R, G, and B bands corresponded to standard color filter bands. For a projector with this optical system, an efficiency improvement of 2.7 is predicted relative to a single panel projector with bandpass color filters and microlenses, assuming perfect aperture ratio recovery in the baseline projector, which is far from the case.

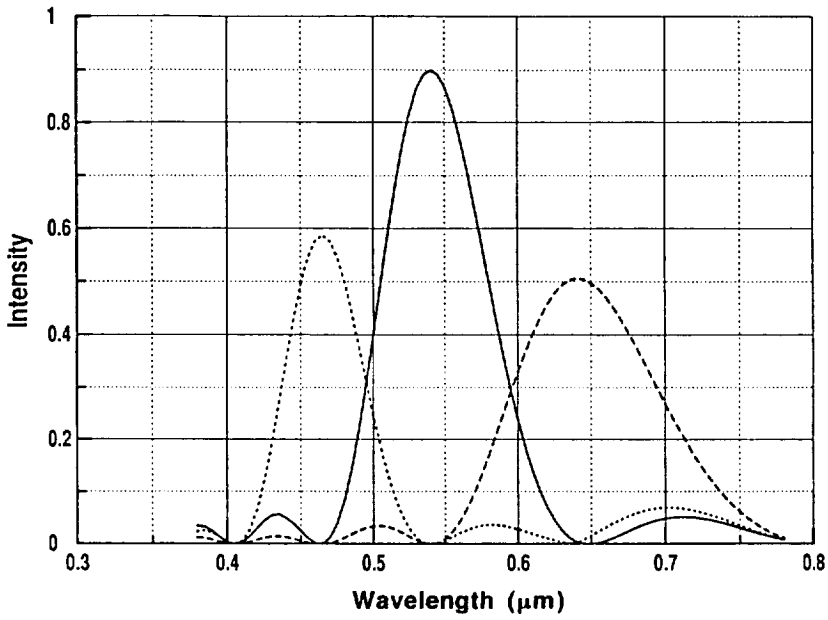

Fig. 18 Color band intensities for each color cell using a 1 mm arc, a 14 μm period grating with six steps, a LC display with a 30 μm pitch and 70% fill factor.

3. Optical Component Characterization and Processing

In the previous section, interactions between individual projector components were discussed, and a model was presented which allows for the calculation of overall system efficiency and spectral output. In this section, key components of the actual projector are introduced, and methods of characterization, manufacturing techniques, and availability are presented.

3.1. *Illumination Source*

In order to evaluate collimation properties of commercially available illumination sources the following experiment was performed. An iris aperture of 2.3 cm diameter was placed in front of each illumination system, consisting of lamp, reflector and collimation lens. The iris was placed at a distance of 34.5 cm from the lamp arc gap and its height was adjusted to the axis of the illumination system. Only the beam passing through the aperture was propagated onto a screen over a distance of ~ 2 m, i.e., over a distance large with respect to the aperture diameter. The experimental setup is schematically drawn in *Fig. 19*. A photo diode/digital oscilloscope combination was used to map out the relative intensity variations within the projected lamp spot for each of the three wavelengths, red = 610 nm, green = 575 nm, and blue = 437 nm. Evaluation of the data showed that typical divergence angles of conventional illumination sources, mostly quartz halogen lamps with parabolic reflectors, were between 16° and 19°. Since the constraint analysis given in the previous section indicated reduced color saturation and the need for high speed microlenses as the divergence exceeds 3°, conventional available collimated quartz halogen lamps were found to be unsuitable as illumination sources for the echelon grating / microlens color separation concept.

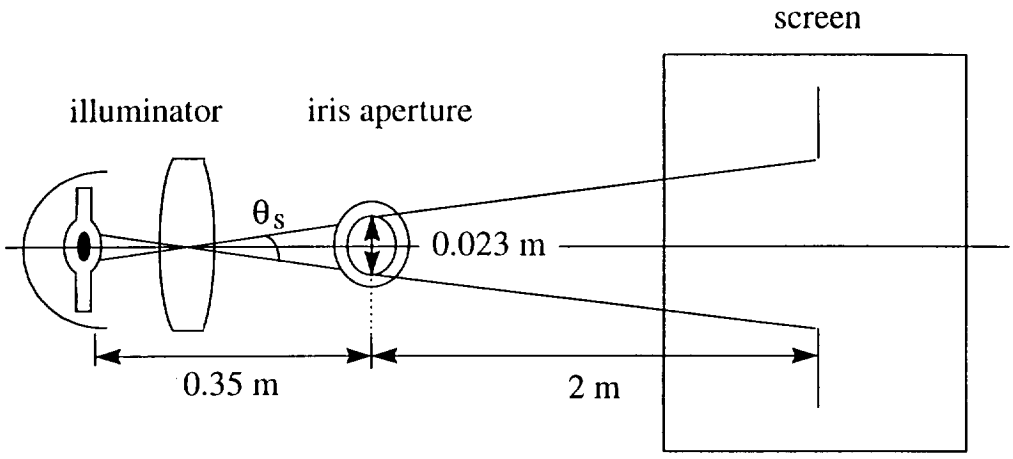

Fig. 19 Setup for the evaluation of source collimation properties.

Preliminary screening of other short arc lamps (Xe arc, Xe-Hg arc, metal halide arc) indicated that metal halide lamps did not only provide the highest spectral brightness, but with the use of a spherical reflector and appropriate condenser, achieved reduced beam divergence compared to conventional quartz halogen systems. Also, the spectral emission of a metal halide lamp occurred in bands located mostly in favorable parts of the visible spectrum and could within limits be tuned to a specific application. Rockwell identified two sources for metal halide lamps The first was ILC Technology, Inc., Sunnyvale, CA, the second was Sharp Corp. A custom lamp / reflector assembly was provided by ILC for evaluation. The final vendor choice, however, was Sharp since the illumination source of the benchmark Sharp projector was better collimated than the ILC illuminator and was already fully integrated into a projection system. The Sharp illumination system included a small metal halide lamp, reflector, correction element and condenser lens. A relative intensity map of the lamp arc (*Fig. 20*) showed the emission was confined to a region not much greater than 3 mm. The total angular divergence of the illuminating beam was measured to be 6°. The emission spectrum was measured with an optical multichannel amplifier and corrected for the spectral response of the instrument, *Fig. 21*.

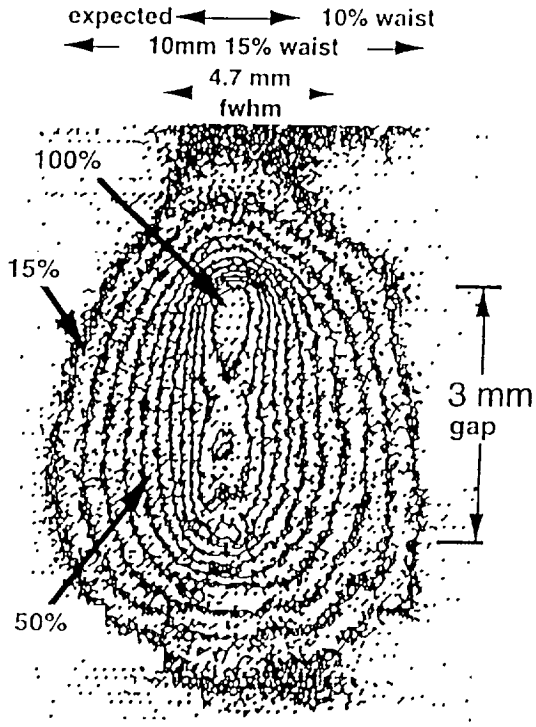

Fig. 20 Image of the metal halide lamp arc showing that the emission is restricted to an area of ~ 3 mm.

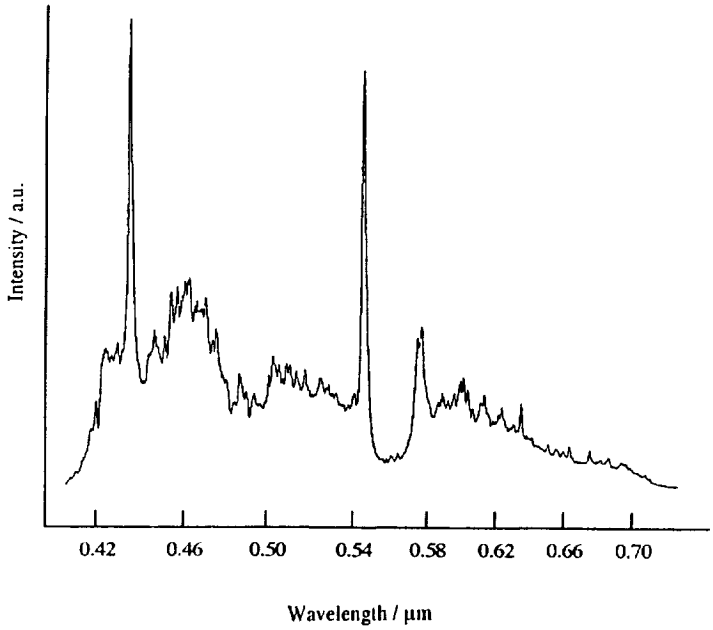

Fig. 21 Spectral emission of the Sharp metal halide lamp.

Though suitable for the initial overall optical concept validation the Sharp illuminator (BQC-XVP10U//1) limited the maximum echelon grating period and with it the overall efficiency of the projector to values below those of the baseline Sharp projector. If realistic substrate thicknesses, larger grating periods with better diffraction efficiency and smaller pixel sizes in line with the industrial trend are to be realized, illumination systems with 1 - 2 mm arcs must be used. Two sources were identified which fulfill the collimation requirements crucial to improvements of the existing system. The first source, designed by Phillips, presents a breakthrough in metal halide lamp technology.[6] The lamp features an arc length of <1.5 mm, high brightness and a long lifetime of ~ 4000 hrs, more technical information can be found in Table 5. This lamp and collimation system is sold as an integrated unit. It is expected that this system will become more available for evaluation in the near term. An alternative test source with small arc dimension is a high pressure Xe arc lamp with an arc length of 1.14 mm. Its spectral efficiencies, however, are lower and its spectral output in the visible is flat compared to a metal halide lamp.

3.2. *Echelon Grating*

The initial optical design and illuminator choice required a 4 mm grating period which was the minimum that can be supported with available microlithographic processing methods. A brief description of the fabrication process and characterization is given in the following sub-sections.

3.2.1. Echelon Grating Fabrication

See MIT/LL report for detailed information about grating processing methods and constraints, see Appendix B. A schematic diagram of the process is found in *Fig. 22*. A binary optics "echelon" grating structure was fabricated in fused silica. The specifications were formulated in discussions between Rockwell and MIT/LL. The overall dimensions

were determined by the display to be 75 mm x 60 mm (96 mm diagonal). The grating period was set at 4 μm, based on source lamp characteristics. The four level (step) gratings were fabricated in 100 mm diameter fused silica wafers (25 mils thickness) using a binary optics process. For a design wavelength of 0.25 μm and an index of refraction of 1.46, each of the 1 μm wide steps was 1.14 μm deep, for a total etch depth of 3.42 μm.

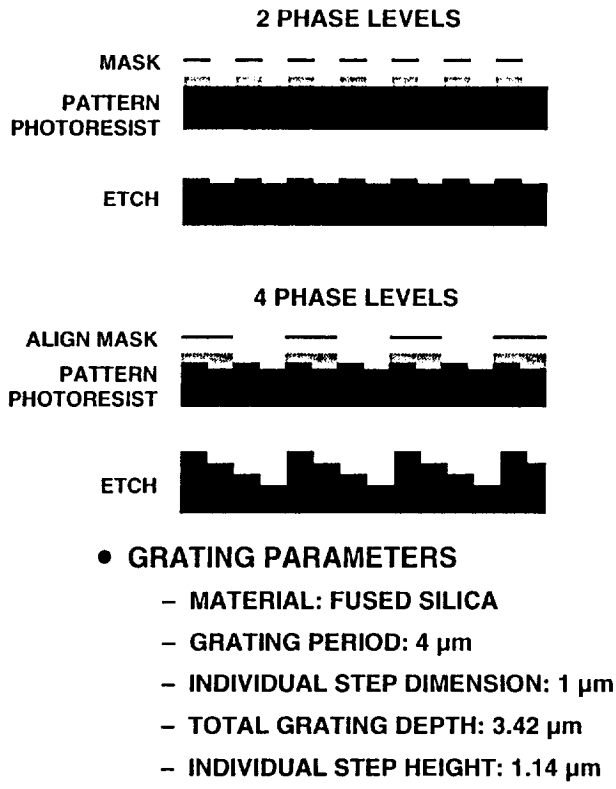

Fig. 22 Schematic diagram of the process flow for fabricating a 4-phase-level echelon grating. Two cycles of photolithography and etching are required.

The gratings were fabricated at MIT/LL Microelectronics Laboratory using 4" silicon-processing equipment. As might be expected, great ingenuity was required to process the transparent, non-conducting fused silica wafers without modifying the silicon-based equipment. Aluminum-coated fused silica wafers were exposed on the 5x reduction I-line optical stepper. Four rows of five 15 mm square grating blocks were exposed across the wafer to create the 75 mm (x) x 60 mm (y) continuous pattern. Stitching errors in the y-

direction ranged between 0.2 and 1 μm. Stitch control of both exposure and development parameters were needed to achieve the 50% duty cycle required by these binary optics gratings. The first mask layer (2 μm period grating) used a 1 μm thick positive photoresist and a 2 μm thick photoresist was used for the second mask layer (4 μm period grating). Thicker resist was needed to planarize the previously etched 1.14 μm deep structures. Overlays better than 0.2 μm (0.15 μm +/- 0.1 μm for a test pattern) were achieved on the stepper using global alignment across the 4" wafer.

Following a wet chemical Al-etch, the substrates were mounted on 4" Si carrier wafers and then etched in a parallel-plate reactive ion etching (RIE) system to the target depth. To achieve the desired anisotropic profile, samples were etched at 20°C in a CF_4/CHF_3/He mixture at a pressure of 300 mTorr and RF power of 350 W at an etching rate of about 62 Å/sec. Selectivity between the photoresist mask and the quartz substrate was approximately 4:1. Etch depths were controlled by etch time. In an initial attempt to monitor the RIE process, the etch depth of 25 μm wide witness etch features was measured at locations adjacent to the grating area with a stylus profilometer. However, an enormous variation (>20%) in the etch depth between the outer 10-15 mm at the wafer's edge (where the witness etch features were located) and the rest of the 75 mm x 60 mm pattern created difficulties in a achieving the desired etch depth. To overcome this, test samples consisting of 15 mm x 60 mm grating stripes having witness etch features adjacent to each stripe were etched and measured. These samples were used to calibrate the RIE process prior to etching the actual 96 mm diagonal gratings.

The performance of the echelon grating was modeled using both simplified scalar and rigorous EM diffraction calculations, as shown in *Fig. 23*. The EM calculations performed at MIT/LL assumed TE polarization and normal incidence (TM polarization results are slightly worse). Because the grating depths for the echelon are significant, and the lateral dimensions are comparable to the wavelength, Lincoln Laboratories expected 50-60%

efficiency as predicted by EM calculations instead of the 80-90% efficiency predicted by scalar theory. The effects of processing variations on grating performance have also been modeled. The simulations indicate that etch depth errors must be less than 3% of the minimum step height for the device to function well. Variations in etch depth shift the center frequency to shorter wavelength if the grating is too shallow and to longer wavelength if the grating is too deep.

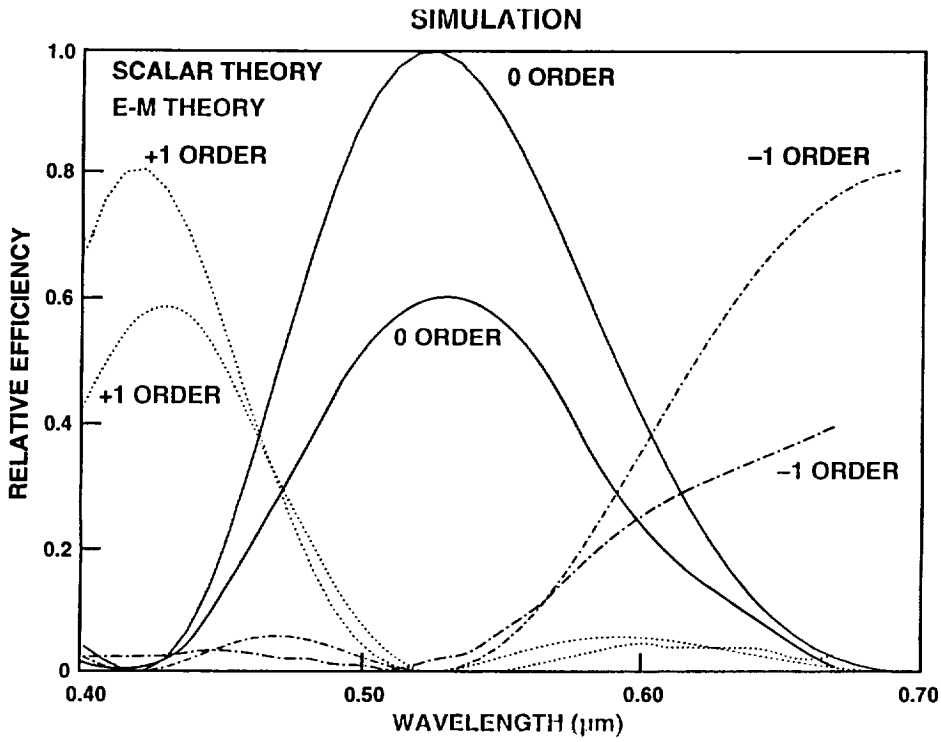

Fig. 23 Simulation of the efficiency of color separation in the scalar approximation (upper lines), and in the more exact electromagnetic vector representation (lower lines). The reduction in efficiency is due to the echelon dimensions, which in the current design are comparable to the wavelength.

3.2.2. Echelon Grating Color Separation Uniformity, Quality and Efficiency Evaluation

For the evaluation of MIT/LL echelon grating color separation uniformity and quality, the collimated beam of a tungsten lamp was passed through each quadrant of the 4 x 5 echelon grating array, dispersed with a monochromator and detected with a

photomultiplier. The signals were digitized and transferred to a computer for further analysis. Quadrants not illuminated during the measurement were covered with a black mask. The spectra collected for each grating order (0, +1, -1) were corrected for the emission spectrum of the tungsten lamp and the spectral response of the detection system. In order to evaluate the efficiency of the echelon grating for generating RGB bands according to industrial color standards the collimated light beam of the tungsten lamp was passed through red, green and blue standard color filters. The transmission through each filter was measured with a photodiode and recorded with a digital oscilloscope. The echelon grating was then inserted into the beam path and the loss of transmission for red, green and blue monitored for each grating quadrant.

The first prototype four step 4 μm period grating dispersed the light into bands that were not well spectrally separated and did not match the standard red / green / blue filter transmission curves. The blue band was centered at 400 nm and red at 700 nm. For later gratings the three bands were well defined and in closer agreement with the calculations, see *Fig. 24*. These gratings also showed greatly improved uniformity, though the center wavelength for each color still shifted ~ 10 - 20 nm to the red from the center to the edges of the grating array accompanied with a 20% drop in efficiency. Overall intensity losses were incurred due to presence of higher grating orders. In addition, most gratings had clearly visible vacuum chuck marks which were imprinted onto the wafer during processing. The prototype grating with the best optical characteristics was used initially to validate the color separation concept using a static aperture mask as described in the following sub-section. The same grating was later installed in the prototype projector.

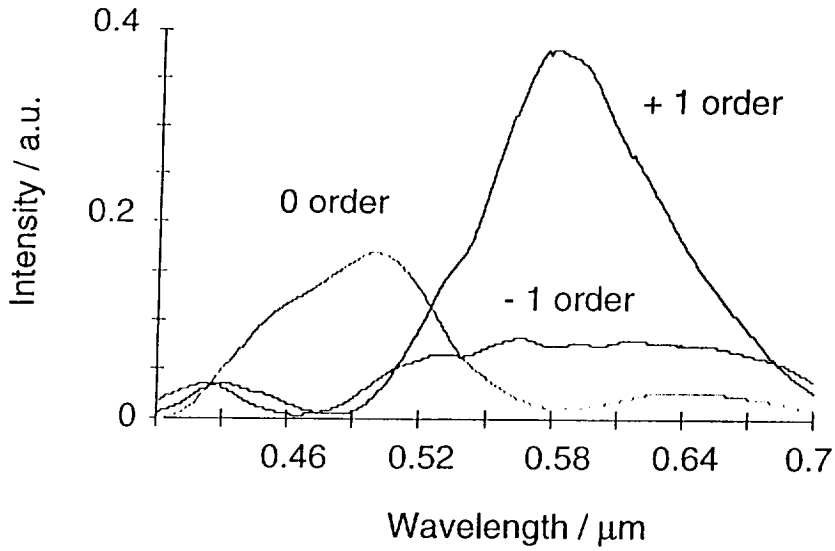

Fig. 24 Measured transmission spectra for zero, + and - first orders of the first MIT/LL echelon grating, illustrating poor color separation.

3.2.3. Concept Validation for Color Separation with an Echelon Grating / Microlens Pair

Preliminary evaluation of the color separation at MIT/LL fully validated the echelon-based color separation concept. The central zero order transmitted blue-green light, with the red diverted into the -1 order and the blue diverted into the + 1 order. The grating operation was observed using a transmission microscope and a microlens array. The microlens array (either 200 μm ~ F/2 photoresist lenses or 500 μm diameter F/4 Coring SMILE lenses) was placed on top of the grating which was illuminated from below. Color was analyzed via a series of color filters placed over the light source.

Echelon grating/microlens pair performance evaluations at Rockwell initially used a static mask to simulate the RGB pixel pattern of the selected Sharp LCLV panel. The mask was bonded to a piece of standard display substrate glass to optically simulate the geometry of the actual display. The central area of the mask simulated an LCLV in the white state with all color dots open, while other areas had patterns consistent with red, green or blue pixels that were turned on or off. This pattern is illustrated schematically in *Fig. 25*. When combined with the grating and microlens array, the mask acted exactly as an LCLV with a static pattern, allowing complete optical characterization without the

need to have a fully functional LCLV. *Figure 26* presents a photograph of the completed mask. The overall optical concept was demonstrated using the Sharp illuminator, echelon grating, microlens array, static aperture mask, and projection lens. Based on the diffraction characteristics, the first grating was not expected to give accurate color rendition. However, as shown in *Fig. 27,* the demonstration did illustrate that the overall optical scheme was functioning as predicted. This figure displays a projected image of a portion of the illuminated static mask. The area illuminated was divided into three regions. The region on the right represented a primary color (in this case red) and the region on the left was divided into an upper region representing a secondary color (amber) and a lower region representing white. The actual colors were not well reproduced, but the color difference between the three regions was evident and agreed with predictions based on the actual performance of the grating. *Figure 28* is a photograph of the resulting projected image; Fig. 28a gives a description of the expected color content. The colors are well separated. Scanning the microlens demonstrated a capability to change the projected color through the primary and secondary regions of the aperture mask, as predicted.

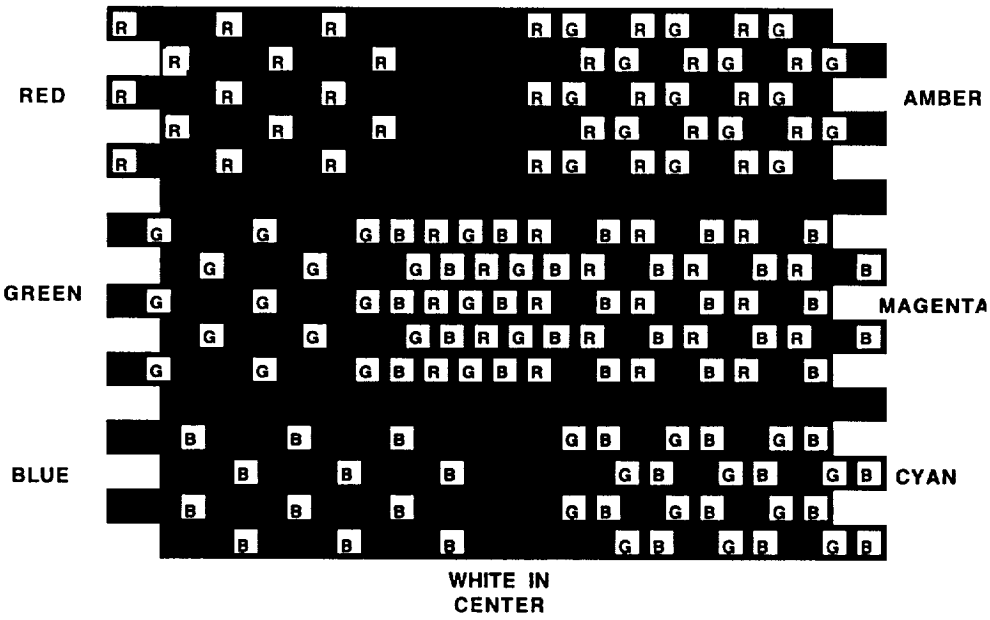

Fig. 25 Patterned static LCLV simulation mask.

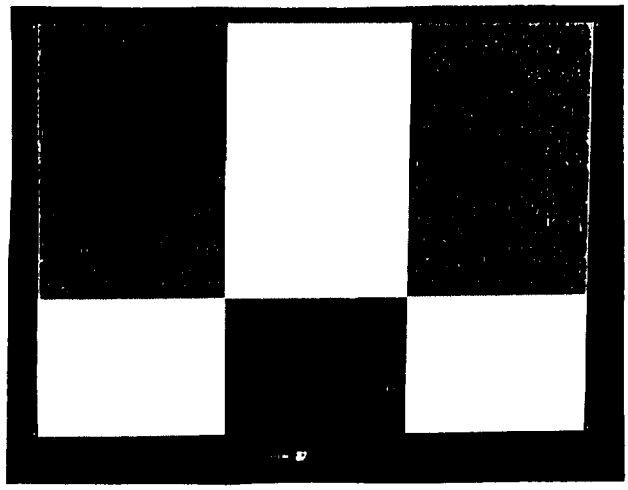

Fig. 26 Photograph of completed LCLV simulation mask.

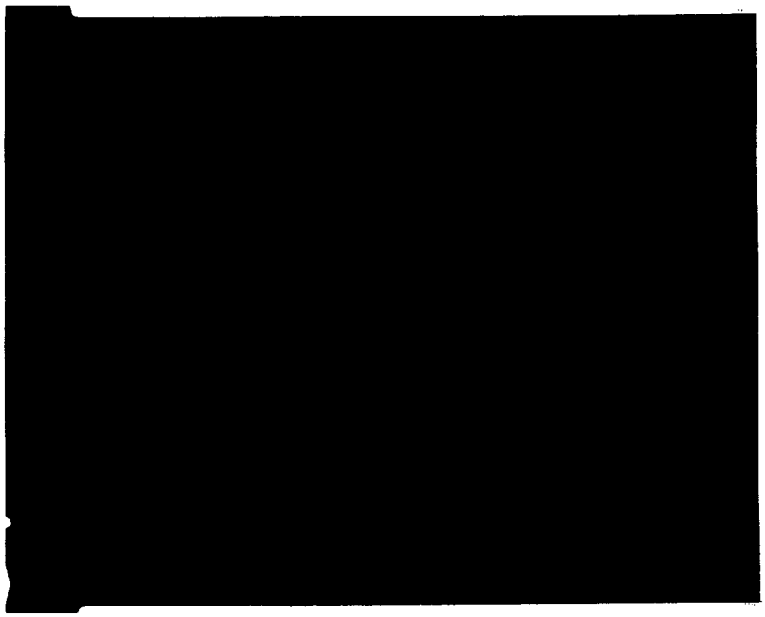

Fig. 27 Photograph showing the color separation achieved with the first MIT/LL echelon grating, refractive microlens array with black mask, and static LCLV aperture mask. The right portion of the scene is designed to transmit a primary color. The left portion of the scene is divided into two regions, the upper transmitting a secondary color (two color pixels are transmitting) and the lower transmitting white (all three pixels transmitting).

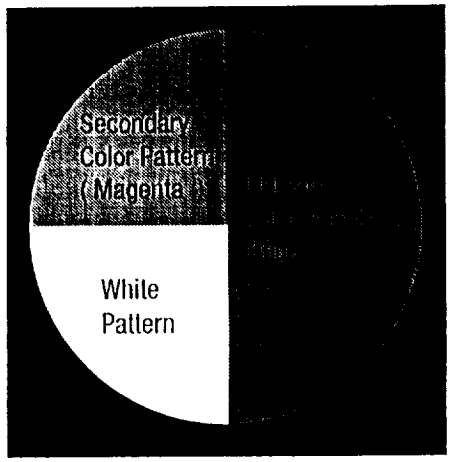

28 a

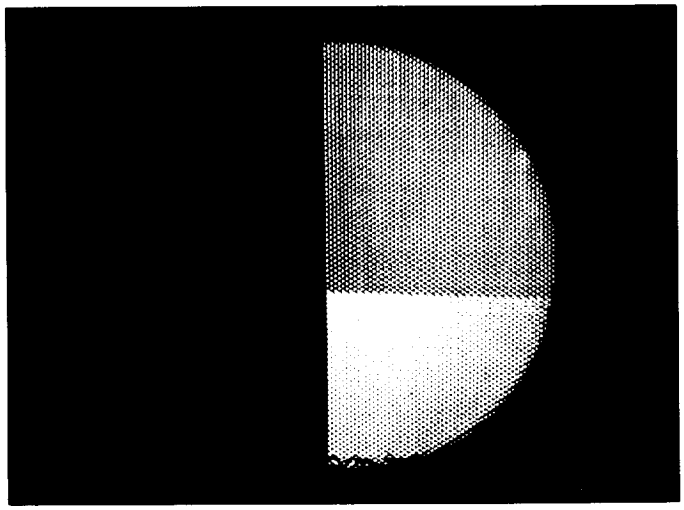

28 b

Fig. 28 Demonstration of color separation in a projection LCLV configuration. The area that is shown represents a small region of the static aperture mask. Figure 28a indicates the expected colors that are produced by the areas having single color clear apertures (primary color), two color clear areas (secondary color) and all three color apertures clear (white). The improved grating produces the expected color separation spectra. Figure 28b is a photograph of the actual projected image.

Adjustment of the spectra of the differential beams to match required red / green / blue standard color filter bands would require increasing the number of grating steps to reduce the spectral separation of RGB bands. For example, a six step echelon grating would center the red and blue bands at 450 nm and 650 nm respectively, as compared to the 440 nm and 680 nm for a four step, 4 μm period grating. The impact on the system chromaticity is illustrated. It is easily seen that increasing the number of steps to six brings the maxima of the R, G, and B bands closer together. Since the current design features a four micron period grating, increasing the number of steps would require submicron processing and would have a further negative impact on grating efficiency. This would be extremely stressing on such a large scale wafer (3.6" diagonal). However, if the grating period can also be increased, then adding more grating steps becomes practical. A larger period grating is not feasible with the current source due to its large arc size, which again stresses the importance of identifying a lamp with a suitably short arc.

3.3. *Microlens Array*

The echelon grating color separation concept requires refractive rather than binary optic microlenses to avoid chromatic aberrations and to couple the angularly deviated spectrally dispersed beams to the correct display dots. In addition to an investigation of the availability of these components from other vendors, Rockwell has developed methods to fabricate refractive microlenses suitable for this and other applications under internal funding.

The method for fabricating refractive microlenses uses a single mask level process. A detailed description of the process can be found in Science Center publications in SPIE proceedings.[7] An abbreviated process outline will be given.

A photoresist pattern is created on an appropriate substrate in the form of circular islands. The substrate is then heated until the photoresist flows. Surface tension causes the resist to take a nearly spherical lens profile. The part is then etched using reactive ion etching,

thus transferring the refractive lens structure into the substrate material. An example of one such array is depicted in *Fig.29*. The measured lens f-number was 4.2, compared to a target value of 4.27. The next step in microlens processing is to incorporate an optically opaque mask layer between the microlenses.

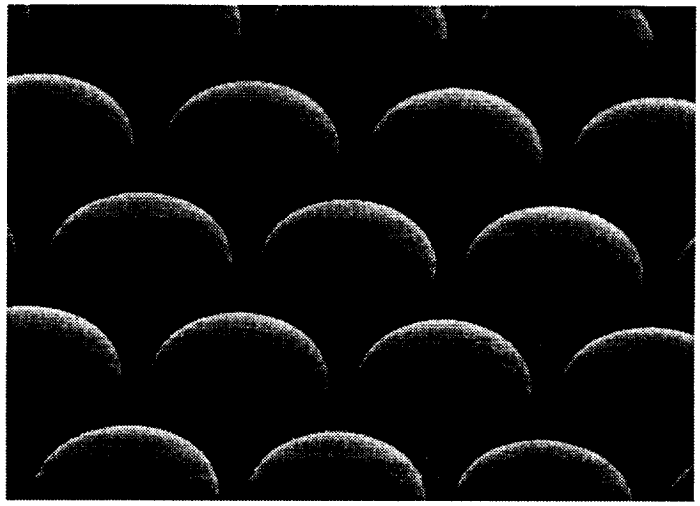

Fig. 29 Refractive microlenses fabricated in quartz using the photoresist reflow and reactive ion etch process have a measured f/number of 4.2, compared to the design goal of 4.27.

Currently, internally funded efforts are under way to develop methods for processing rectangular microlenses for a variety of applications. These arrays would allow a fill factor close to 100%, a larger degree of freedom with respect to design choices, and would not require a black matrix to cover the inactive areas of the array.

4. Prototype Projector

Rockwell's Collins Avionics and Communications Division successfully modified a Sharp single panel liquid crystal projector, integrating an echelon grating and microlens array to enable a complete demonstration of our color separation concept. The LCLV in the Sharp projector has an integral microlens array to increase the effective aperture ratio (the aperture ratio of the amorphous silicon panel was only 27%). This microlens array has one microlens over each color

dot. The microlens array required for our color separation concept has one microlens to every RGB color group. Modeling and experiments indicated that the Sharp microlens array could be left attached to the panel if the panel were reversed such that the microlens array faced the projection lens. However, reversal of the panel results in image distortion, so the decision was made to remove it. During the microlens removal process, it was discovered that the LCD panel was actually monochrome with a color filter array incorporated into the microlens structure. While not initially intended, the use of a monochrome panel enabled visual evaluation of the color gamut produced by the micro-optic assembly alone. Installation of our microlens array and grating was performed by building mounting standoffs from the LCD panel frame. The small additional volume occupied by the micro-optic elements eliminated the need for any further modification of the projector optical system. *Figure 30* shows the LCD panel with the microlens and grating arrays installed, the open projector, and the assembled modified projector. In the process of modifying the panel, the flex circuit for half of the rows was damaged making half of the panel inoperable. Nevertheless, the projector was successfully demonstrated at the DARPA HDS, IEC meeting in Washington '95 and exhibited good color separation, but processing defects in the grating, such as step and repeat pattern and vacuum chuck imprints, were visible in the projected image.

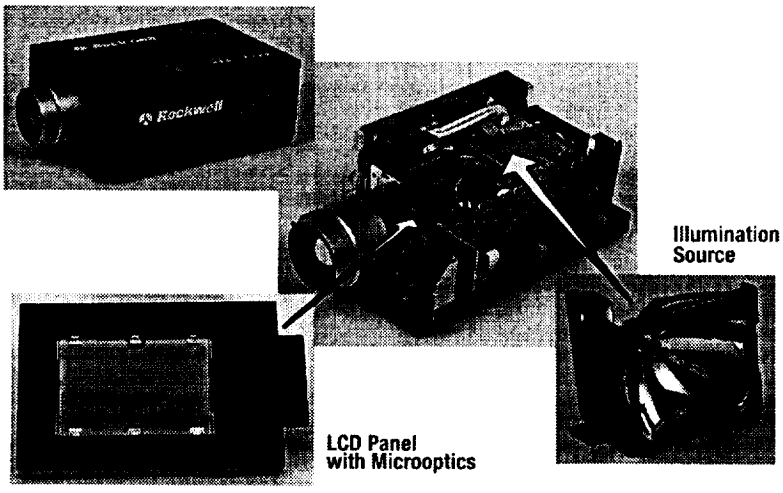

SCP0653C.042895

Fig. 30 LCD panel with microlens array and echelon grating installed, lamp assembly and assembled projector.

The color balance of the demo projector compared to the NTSC standard was measured by Rockwell Collins, and the data are presented in Table 5. Color saturation was not ideal, the green transmission was desaturated due to contributions from higher order diffraction bands, and the red transmission was weak due to the four step grating design which produces too great a spectral separation between the red and blue bands. The measured chromaticity performance (1976 CIE Standard) of the projector is shown in *Fig. 31*. Red, green and blue field spectral distributions are given in *Figs. 32* through *34*. The luminance performance relative to green was measured, as well as the reflected luminance on screen performance. The results are presented in *Figs. 35* and *36*. Replacing the current grating with a six step design would produce better red– blue separation. Desaturation can be addressed by including a color filter array in the panel to eliminate spectral crosstalk. In this case, lower saturation color filters (with higher transmission) could be used. The projector, given the constraints of the available lamp and resulting 4 micron pitch grating, did not have an efficiency improvement over the unmodified display. It did, however, demonstrate the color separation concept to be valid and elucidated areas where significant efficiency gains are possible pending availability of a more highly collimated source.

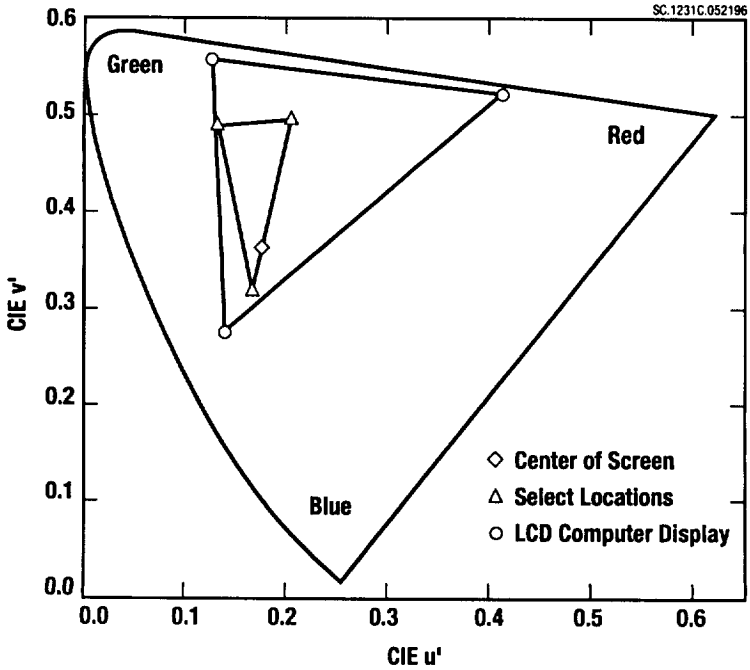

Fig. 31 Micro-optic/Echelon grating projector chromaticity performance.

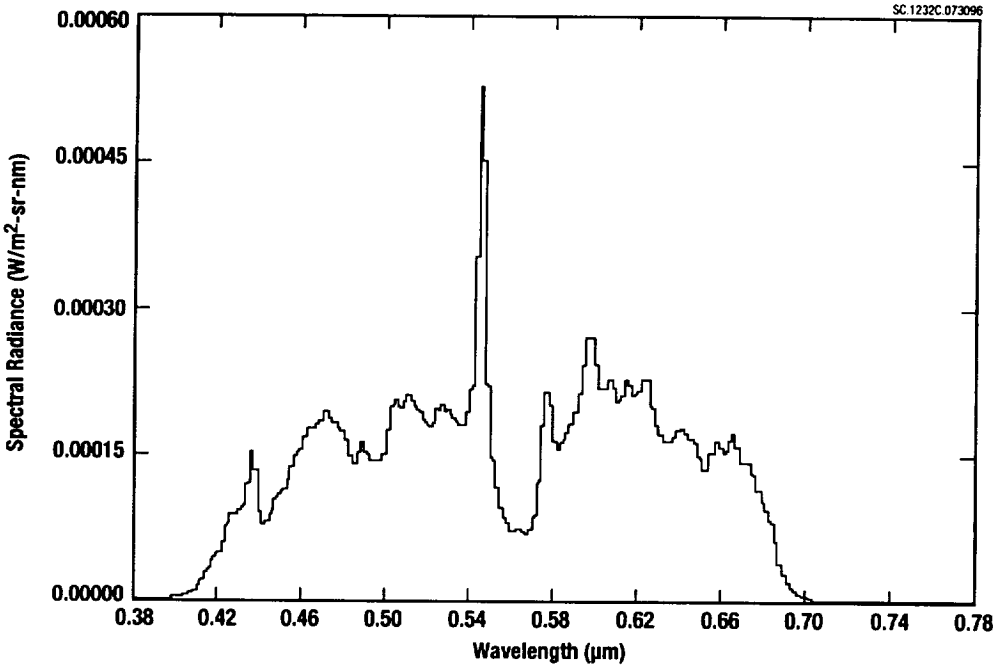

Fig. 32 Projector relative red field spectral distribution.

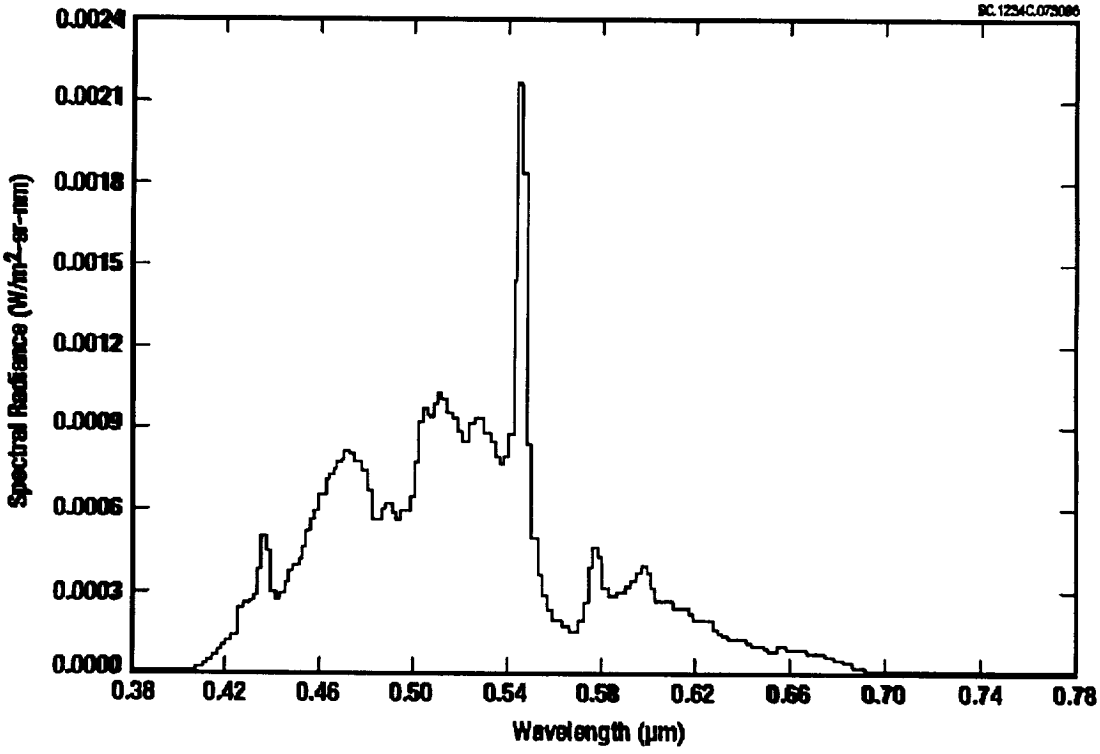

Fig. 33 Projector relative green field spectral distribution.

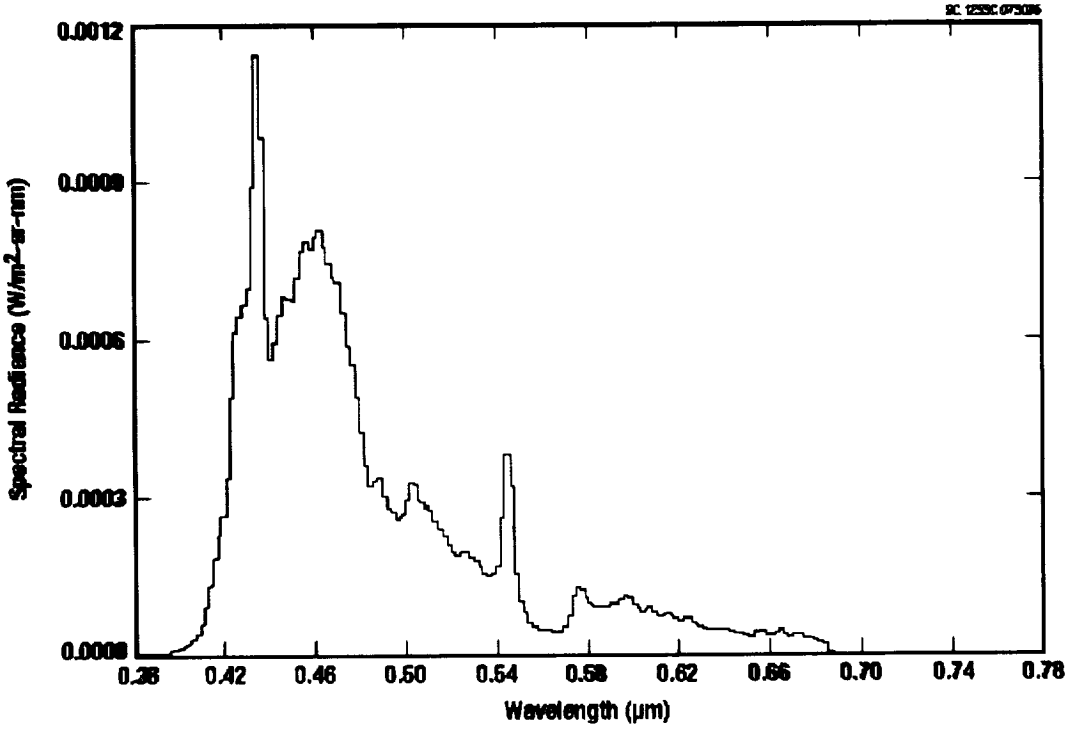

Fig. 34 Projector relative blue field spectral distribution.

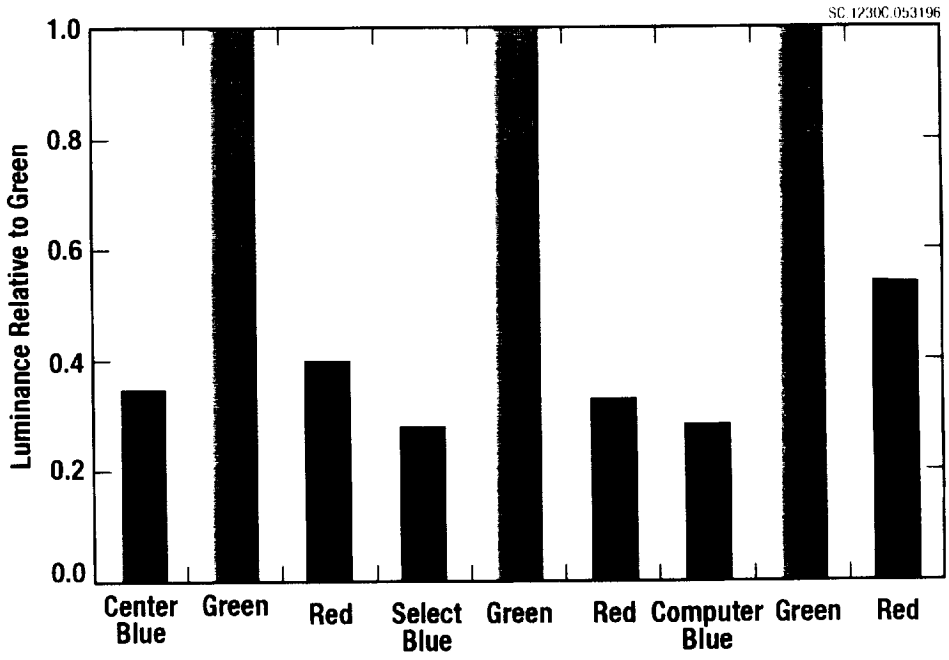

Fig. 35 Luminance performance relative to green.

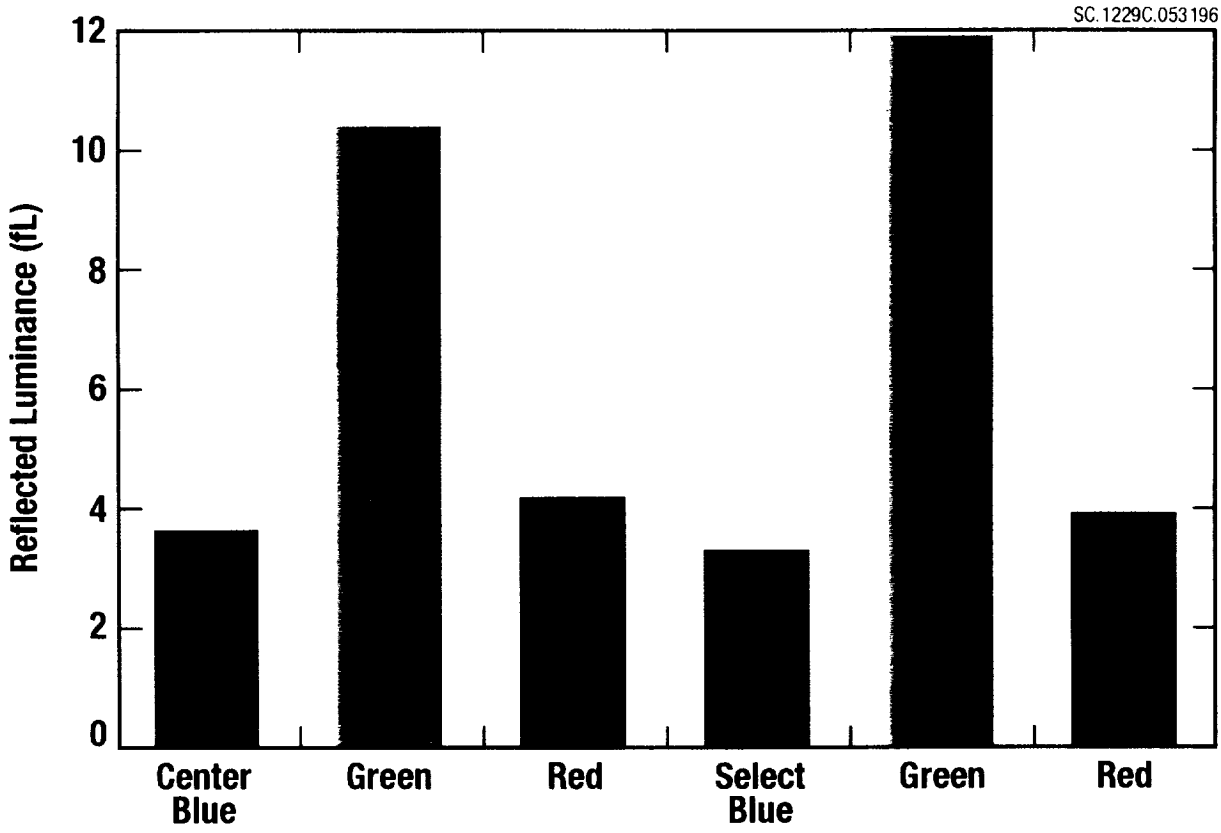

Fig. 36 On-screen performance, reflected luminance.

5. Summary and Recommendations

During phase I of this program, efforts focused on design, modeling and demonstration of a full-color single panel liquid crystal projector that used a micro-lens/echelon grating combination for color separation. An optical projector baseline design was developed based on constraints imposed by microlens manufacturing techniques, commercially available LCD panel layouts and illumination system properties. The use of round refractive microlenses to direct color bands to the appropriate color pixels was compatible only with a delta triad color pixel pattern and yielded a maximum fill factor of ~ 85%. Commercially available metal halide illumination systems with typical arc lengths of ~3 mm and a total beam divergence of ~6 °–10° restricted the echelon

grating design to a 4 μm period with four steps with subsequent low efficiency. Rockwell/Collins identified Sharp panel No. LQ46E02 as best suited to satisfy constraints imposed by light valve pixel width (114 μm) and substrate thickness (1.28 mm). The panel was assumed to have a clear aperture ratio of 50%.

An end-to-end model to predict color output and efficiency of the baseline projector as a function of key optical component parameters was developed. The performance of the projector with a 3 mm arc, a 4 μm four step grating, a clear aperture ratio of 50% and a cell width of 114 μm was predicted to be 60% in the green, 28% in the red and 23% in the blue. The calculated location of the color bands did not accurately overlap with standard color filter bands optimized for eye response. The model was then used to predict areas for system improvement by calculating color output and system efficiency as a function of decreasing arc length, varying clear aperture ratios and increasing grating periods. Modeling results showed the maximum grating period to be critically dependent on arc length. More efficient, larger grating periods were shown to require short arc lengths of ~ 1-2 mm. In turn, larger grating periods would enable the use of smaller pixels. An ideal system was proposed with an illumination source with a 1 mm arc, a 14 μm period six step grating, 70% fill factor and 30 μm cell width. The color rendering of this system was identical to that of standard color filters. The calculated efficiencies were 90% in the green, 59% in the blue and 50% in the red.

Selected optical components were used for a demonstration of the color separation concept. The best available illumination system with respect to beam divergence, intensity and color rendering at the time was a metal halide lamp from Sharp with an arc length of ~ 3 mm and a total beam divergence of 6°. The selection of the best echelon grating made by Lincoln Laboratories was based on measurements of color separation, uniformity, quality and efficiency. Even the best gratings showed visible fabrication defects such as vacuum chuck imprints and stitching offsets. Efficiency dropped by 20% from the center to the edge of the gratings due to process variation and diffraction into the higher orders. The color rendering of the best gratings, however, was in

agreement with theoretical predictions. Rockwell/Collins incorporated a selected echelon grating/microlens array combination into a commercial Sharp liquid crystal projector. Integration of the Rockwell / MIT/LL components required only minor changes to the projector and no extra space. Chromaticity performance, color field spectral distributions and luminance performance were measured by Rockwell/Collins and were consistent with results obtained by modeling.

The measured and modeled overall performance of the prototype projector as a function of design parameters lead to the overall assessment that illumination source arc length has a dramatic impact on overall system efficiency. Using a source with a 3 mm long arc the projection system is restricted to a 4 μm, four step grating. This intrinsically has such a low efficiency that it shows no improvement over the Sharp baseline projector. A more detailed discussion of areas for improvement is given below.

The initial design was laid out for a LCLV panel with a clear aperture ratio of 50%, while the actual Sharp LCD panel used for the prototype projector had a measured effective aperture ratio of only ~ 27%. *Figure 17* clearly shows how a reduction of the aperture ratio from 50% to 27% impacts the efficiency of the overall design due to blocking experienced by all three colors (efficiency reduction of 55-60%). Consequently, the LCLV should be replaced with one having a better aperture ratio or the microlens array properties should be adjusted appropriately to optimize the fill factor. To achieve an ideal fill factor of ~ 100% microlenses with rectangular apertures must be used. Such microlenses would also eliminate the need for a black matrix layer to obscure the areas not covered by microlenses which is a complicating factor for inexpensive replication of the microlenses.

The pixel size of the selected Sharp LCLV was ~ 114 μm. It is highly desirable to use smaller, higher resolution LCLVs that are more in line with the current industrial trend. Such panels, however, cannot currently be supported due to restrictions imposed by the collimation properties and arc source dimension of the illumination source. Detailed system analysis showed that an illumination source with an arc length of 1–2 mm would enable the use of smaller pixel

widths. The results of these calculations were very encouraging and the impact of arc length on system efficiency could be demonstrated with Xe high pressure short arc lamps which are readily available with very short arc lengths of ~ 1.14 mm. In the longer term a new metal halide lamp developed by Phillips is expected to become available. This metal halide lamp has the desired short arc length of 1 - 2 mm, integrated collimation optics and a surprisingly long life of > 4000 hrs.

Shorter arc lengths are the key to smaller pixel sizes and the use of larger period echelon gratings which could increase the efficiency of the projector by ~ 20% in the blue and up to 40% for red and green. Longer period gratings have a higher diffraction efficiency into 0 and +/- 1 orders (~30% improvement from a 4 μm four step grating to a 14 μm period, six step grating) and, in addition, would be easier to produce. Future production methods for echelon gratings need to address echelon grating manufacturing problems that were encountered during Phase I of this project, such as stitching errors, patterns left behind by the vacuum chuck, and uniformity variation.

6. Tables

Table 1

Brightness improvements over the Sharp low-cost projector

	Ideal	Now (% of ideal)	Future**
Grating/ML	300%		
grating efficiency	100%	60%	85%
grating dispersion	100%	85%	100%
microlens fill factor	100%	5%	100%
Filter*	200%		
With filter in	300%	130%	255%
With filter out	600%	260%	510%

* Current filter transmittance is uncertain (assumed T = 0.5)

** Future estimates depend on a smaller arc lamp (< 2 mm) and rectangular or square microlenses

Table 2

Sharp display module model No. LQ46E02 mechanical specifications

Parameter	Specifications	Unit
Display format	EVEN LINE 643 (H) x 240 (V) ODD LINE 644 (H) x 240 (V)	pixels
Active area	73.3 (H) x 54.7 (W)	mm
Screen size	3.6 (Diagonal)	inch
Pixel pitch	0.114 (H) x 0.114 (W)	mm
Pixel configuration	Delta configuration	-
Outline dimension*	138.7 (W) x 91.0 (H) x 11.0 (D)	mm
Weight	Approx. 150	g

*Including protrusion

Table 3

Sharp LCD projector XV-P10U mechanical specifications

Receiving system	NTSC
Liquid crystal	Single 3.6" (9cm panel)
Drive system	Active matrix thin-film transistor (TFT)
No. of pixels	100, 386 (RGB triad)
Projection lens	f123 mm 1:2.8 fixed focus
Screen size	30" (76 cm) 100" (254 cm)
Projection distance	1 m (3.3') for a 30" (76 cm) image, 3.3 m (10.8') for a 150" (381 cm) image
Horizontal resolution	350 lines
Luminance	250 lux and 30" (76 cm) screen size
Lamp	150W metal halide
Terminals	Input S-video x 1, Video x 2 (RCA), Audio x 2
Power source	120V AC, 60 Hz
Power consumption	175 W
Dimensions (W x H x D)	215 x 149 x 185 mm (8.5" x 5.9" x 15.2")
Weight	4.1 kg, (9.0 lbs)
Wireless remote control	no
Amplifier and speaker	Yes

Table 4

Color separation projection optics design equations

$f_m^{\#} =$	$(t_o + t_s/n) / (1.8\ w_c)$	microlens f/number
$T_g =$	$(1.8\ \lambda\ f_m^{\#})$	grating period
$f_s^{\#} =$	$1.8\ w_s\ f_m^{\#} / (800\ w_c)$	condenser lens
$\theta_s =$	$1 / (1.8\ f_m^{\#})$ (rad) or $100 / (\pi\ f_m^{\#})$ (deg)	maximum beam spread
$f_p^{\#} =$	$f_m^{\#} /2$	projection lens f/number

where:

w_c = color dot pitch (assuming square pixels)
w_s = source width or arc length for a metal halide source
t_o = distance from the microlens focal plane to the LCD substrate
t_s = thickness of the display glass substrate
θ_s = maximum full angle beam spread for the illumination source to avoid color mixing by the grating

Table 5

Projector color balance compared to NTSC standard

Color	Demo Projector	NTSC Standard
Red	0.299	0.509
Green	0.587	1.00
Blue	0.114	0.194

7. Appendix A

BASIC code chroma2.bas that models grating color separation. Output is in gcell, rcell and bcell, which may be read in MP as pcell.

```
defdbl a-z
dim nd as integer
nd%=201
dim Spec(nd%) as Double,Wvs(nd%) as Double
dim np as integer,j as integer
dim SpectrumFactor as Double
dim Iblue(nd%) as Double,Igreen(nd%) as Double
dim Ired(nd%) as Double,Wavelengths(nd%) as Double
dim pi as double,Wave0 as double,CellWidth as double
dim SourceAngleSpread as double,MicrolensFnum as double
dim wvl as double,CellFillFactor as double
dim CellBeamWidth as double
dim Nstep as integer,Nwaves as integer,i as integer
dim m as integer,tmp as double,triStim as integer
dim rfilter(nd%),gfilter(nd%),bfilter(nd%)
declare function Eta(integer,integer,double,double) as double
        pi=4*atn(1)


          '   cls
  Wave0=.540#                          ' Wavelength of zero order
  arcLength=3                          ' Source arc length in mm
  CellWidth=114                        ' Individual color cell in um
        ApertureRatio=.50#             ' Display aperture ratio
  Tg=4                                 ' Grating period [look in eta( )]
  Nstep%=4                             ' Number of steps per period

        MLalign=0                      ' mm translation of microlens DOESN'T WORK YET
        FocalLengthOfCollimator=32.5   ' in mm
    ths=atn(arcLength/FocalLengthOfCollimator)
        MicrolensFnum=Tg/(1.8#*Wave0)
                wc=CellWidth
        F=1.8#*wc*MicrolensFnum
    thAl=MLalign/F : ML=MLalign
    sar2=sqr(ApertureRatio)/2
    cub=1+sar2
    clb=1-sar2
    nxt=clb+1
    print "MFnum.F ";MicrolensFnum:F;F*1.52 ': stop
  Nwaves%=81
  for i%=1 to Nwaves%
        wvl=.38#+(i%-1)*(.78#-.38#)/(Nwaves%-1)
                thc=wvl/Tg        'angle of +1 order
    if F*ths/2<sar2*wc+ML then
        fgg=1    'fraction of wvl in green order in green cell
    else
        fgg=1-2*(F*ths/2-(sar2*wc+ML))/(F*ths)
    end if
```

```
  frg=0
  if F*(thc-ths/2)<sar2*wc+ML then
      frg=(sar2*wc+ML-F*(thc-ths/2))/(F*ths)
  end if
  fbg=0
  if F*(-thc+ths/2)>-(sar2*wc+ML) then
      fbg=(F*(-thc+ths/2)-(-(sar2*wc+ML)))/(F*ths)
  end if
  Igreen(i%)=fgg*(frg*Eta(1,Nstep%,Wave0,wvl)_
                  +fgg*Eta(0,Nstep%,Wave0,wvl)_
         +fbg*Eta(-1,Nstep%,Wave0,wvl))

  fu=0
  if F*(Thc+Ths/2)>cub*wc+ML then fu=(F*(thc+ths/2)-(cub*wc+ML))/(F*ths)
  fb=0
  if F*(Thc-Ths/2)<clb*wc+ML then fb=((clb*wc+ML)-F*(Thc-Ths/2))/(F*ths)
  frr=1-fu-fb
  if F*(thc+ths/2)<clb*wc+ML or F*(thc-ths/2)>cub*wc+ML then frr=0
                  fgr=0 ' fraction of wvl in green order in red cell
  if F*ths/2>clb*wc+ML then fgr=(f*ths/2-(clb*wc+ML))/(F*ths)
  fbr=0 ' fraction of wvl in blue order in red cell
  if F*(-thc-ths/2)<-(nxt*wc+ML) then
      fbr=(-(nxt*wc+ML)-F*(-thc-ths/2))/(F*ths)
  end if          'end of red cell
  Ired(i%)=fgg*(frr*Eta(1,Nstep%,Wave0,wvl)_
                  +fgr*Eta(0,Nstep%,Wave0,wvl)_
        +fbr*Eta(-1,Nstep%,Wave0,wvl)) 'fgg for vertical cuts

  fu=0
  if F*(-thc-ths/2)<-(cub*wc+ML) then fu=(-(cub*wc+ML)-F*(-thc-ths/2))/(F*ths)
  fb=0
  if F*(-thc+ths/2)>-(clb*wc+ML) then fb=(F*(-thc+ths/2)-(-(clb*wc+ML)))/(F*ths)
  fbb=1-fu-fb

  if F*(-thc-ths/2)>-(clb*wc+ML) or F*(-thc+ths/2)<-(cub*wc+ML) then fbb=0
                  fgb=0 ' fraction of wvl in green order in blue cell
  if -F*ths/2<-(clb*wc+ML) then fgb=(-(clb*wc+ML)-(-F*ths/2))/(F*ths)
  frb=0 ' fraction of wvl in red order in blue cell
  if F*(thc+ths/2)>nxt*wc+ML then
       frb=(F*(thc+ths/2)-(nxt*wc+ML))/(F*ths)
  end if          'end of blue cell
  Iblue(i%)=fgg*(frb*Eta(1,Nstep%,Wave0,wvl)_
                  +fgb*Eta(0,Nstep%,Wave0,wvl)_
        +fbb*Eta(-1,Nstep%,Wave0,wvl))

  ' print "wavelh ";wvl;Iblue(i%);Igreen(i%);Ired(i%) : delay .1
                  Wavelengths(i%)=wvl
next i%
   'stop
open "Bcell" for output as #1
open "Gcell" for output as #2
open "Rcell" for output as #3
print #1,Nwaves%
print #2,Nwaves%
```

```
   print #3,Nwaves%
   for i%=1 to Nwaves%
         print #1,Wavelengths(i%),Iblue(i%)
      print #2,Wavelengths(i%),Igreen(i%)
      print #3,Wavelengths(i%),Ired(i%)
   next i%
   close #1,2,3
stop

Function Eta(m as integer,N as integer,wvld as double,wvl as double)
dim pi as shared double    'Diffraction Efficiency
dim arg as local double,sa as local double
dim sn as local double,etar as local double
dim sinc as local double
         sinc=1
   if m%<>0 then
         arg=pi*m%/N%
      sinc=sin(arg)/arg
   end if
   arg=pi*(wvld/wvl+m%/N%)
   sa=sin(arg)
   sn=sin(N%*arg)
   etar=sinc*sn/(N%*sa)
   etar=etar*etar
   if m=0 then etar=etar*.6#        'green
   if m=1 then etar=etar*.59#       'red
   if m=-1 then etar=etar*.42#      'blue
   Eta=etar
End Function
```

8. Appendix B

Color Separation Echelon Gratings, M.B. Stern, G.J. Swanson, J.E. Curtis, MIT/LL

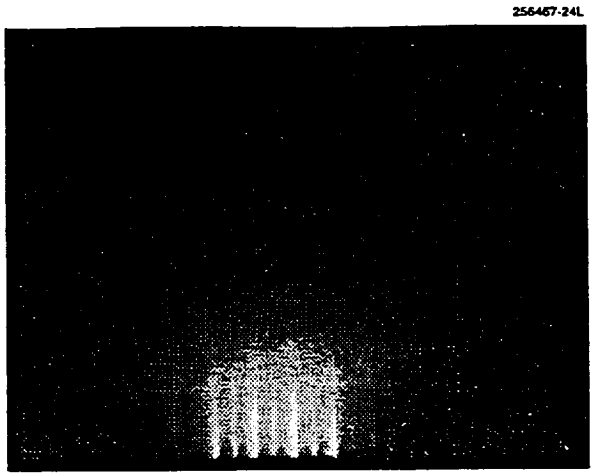

Figure 4-6. 20-keV Reflection electron diffraction pattern from GaN along the [2$\dot{1}\dot{1}$0] direction grown on (0001) sapphire. The substrate temperature is 950°C, and the nitrogen plasma beam is on.

Finally, the significance of this growth regime is evident from the GaN electronic properties. Previous studies have reported that GaN is either residually *n*-type, because of nitrogen vacancies, or insulating and unaffected by intentional doping. We have obtained materials that are residually *n*-type and compare favorably with published results [1],[5],[6] ($n_{300} \approx 2.5 \times 10^{17}$ cm^{-3} and $\mu_{300} \approx 270$ cm^2/V s), as shown in Figure 4-5, and by increasing the gallium flux we have also successfully doped insulating materials with silicon to obtain *n*-type material ($n_{300} \approx 1.2 \times 10^{17}$ cm^{-3} and $\mu_{300} \approx 65$ cm^2/V s). These are some of the highest mobilities reported for silicon-doped GaN grown by ECR MBE. The results suggest that the nitrogen-limited growth conditions reported here will be important for successful *p* doping of GaN, which has proven to be more difficult. Furthermore, these conditions produce high-crystalline-quality material, as shown in the RED pattern in Figure 4-6.

P. A. Maki

4.2 COLOR SEPARATION ECHELON GRATINGS

Color discrimination by wavelength bands has a large number of military and commercial applications. In the infrared portion of the spectrum, wavelength separation allows better temperature discrimination of thermally emissive objects. In the visible portion of the spectrum, a device that separates white light into red, green, and blue wavebands without loss of energy could increase the efficiency of color sensors and color projection displays. As shown in Figure 4-7, an echelon-like grating structure [7] separates electromagnetic (EM) radiation of different wavelengths according to diffraction order rather than by dispersion within one diffraction order as would be the case for a conventional prism-type grating.

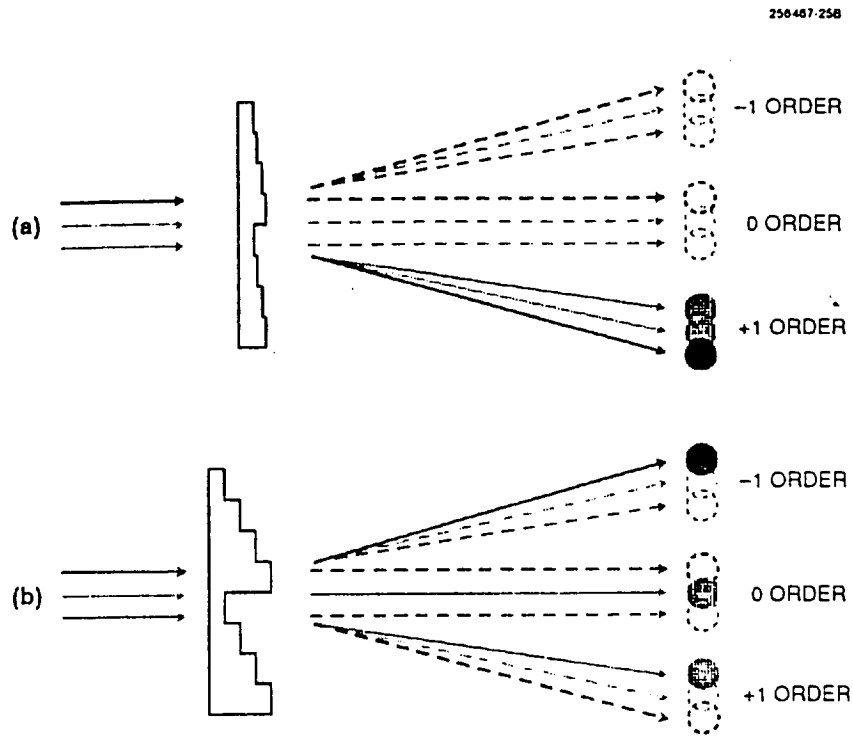

Figure 4-7. Color separation by dispersion in (a) conventional stepped grating and (b) binary optics echelon grating.

A binary optics "echelon" grating structure designed for a color liquid-crystal direct-view projection display has been fabricated in fused silica. This grating disperses red light (700 nm) into the −1 order, green light (525 nm) into the 0 order, and blue light (420 nm) into the +1 order. When combined with a collimated illuminator and a microlens array, it produces arrays of red, blue, and green spots that can be individually controlled by liquid-crystal light valves to form a displayed image.

The echelon grating consists of N steps, each of which has a physical depth $d = \lambda_0/(n_0-1)$, where the grating depth d is determined by the wavelength λ_0 at which the zero-order diffraction efficiency is maximized. The period T is determined by the design wavelength, the number of steps, and the desired lateral separation between wavebands. The display application requires a 75 × 60-mm grating area (96-mm diagonal), a 4-μm grating period, and a four-phase-level profile. The gratings are fabricated in 100-mm fused silica wafers (25-mil thickness) using the binary optics process, which is shown in Figure 4-8. For a design wavelength of 525 nm and an index of refraction n_0 of 1.46, each of the 1-μm-wide steps is 1.14 μm deep, for a total etch depth of 3.42 μm.

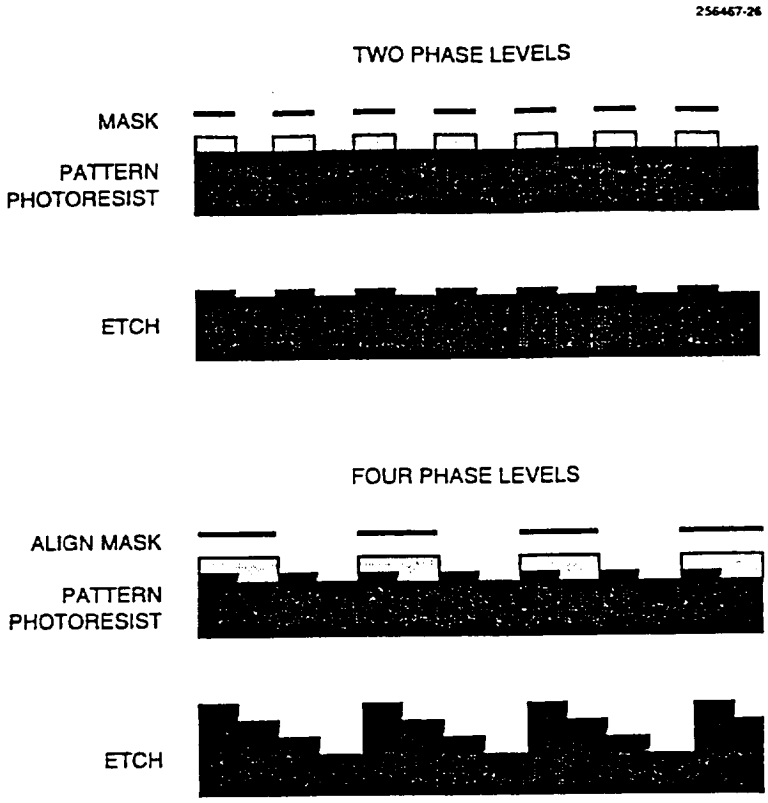

Figure 4-8. Schematic diagram showing two lithographic steps required to fabricate a binary optics component with four phase levels. This sequence can be generalized to fabricate 2^M phase levels using M lithographic steps.

The gratings were fabricated in our Microelectronics Laboratory using the 4-in. Si processing equipment. As might be expected, great ingenuity was required to process transparent, nonconducting wafers without modifying the Si-based equipment. Al-coated fused silica wafers were exposed on the 5× reduction i-line optical stepper. Four rows of five 15-mm-square grating blocks were stepped across the wafer to create the 75 mm (x) × 60 mm (y) continuous patterned area. Stitching errors in the y-direction ranged between 0.2 and 1 μm. Strict control of both exposure and development parameters are needed to achieve the 50% duty cycle required for these binary optics gratings. A 1-μm-thick positive photoresist was used for the first mask layer (2-μm-period grating) and a 2-μm-thick photoresist was used for the second mask layer (4-μm-period grating). Thicker resist was needed to planarize the previously etched 1.14-μm-deep structures. Overlays better than 0.2 μm (0.15 ± 0.1 μm for a test pattern) were achieved on the stepper using global alignment across the 4-in. wafer. (The full coverage of the pattern precluded local alignment.)

Following a wet-chemical Al etch, the substrates are mounted on 4-in. Si carrier wafers and then etched in a parallel-plate reactive ion etching (RIE) system to the target depth. To achieve the desired anisotropic profile, samples are etched at 20°C in a CF_4/CHF_3/He mixture at a pressure of 300 mTorr and RF power of 350 W at an etching rate of about 62 Å/s. Selectivity between the photoresist mask and the quartz substrate is approximately 2.5:1. Etch depths are controlled by etch time. The RIE system can achieve better than 3% uniformity over the central 75-mm-diam region of Si wafers coated with thermal silicon dioxide. In an initial attempt to monitor the RIE process, the etch depth of 25-μm-wide witness etch features was measured at locations adjacent to the grating area with a stylus profilometer. However, an enormous variation (> 20%) in the etch depth between the outer 10–15 mm at the wafer's edge (where the witness etch features are located) and the rest of the 75 × 60-mm pattern created difficulties in achieving the desired grating etch depth. To overcome this, test samples consisting of four 15 × 60-mm grating stripes having witness etch features adjacent to each stripe were etched and measured. These samples were used to calibrate the RIE process prior to etching the actual 96-mm-diagonal gratings.

The performance of the echelon grating has been modeled using the simplified scalar diffraction theory and rigorous EM diffraction calculations, as shown in Figure 4-9. The EM calculations assume TE polarization and normal incidence (TM polarization results are slightly worse). Results are normalized to

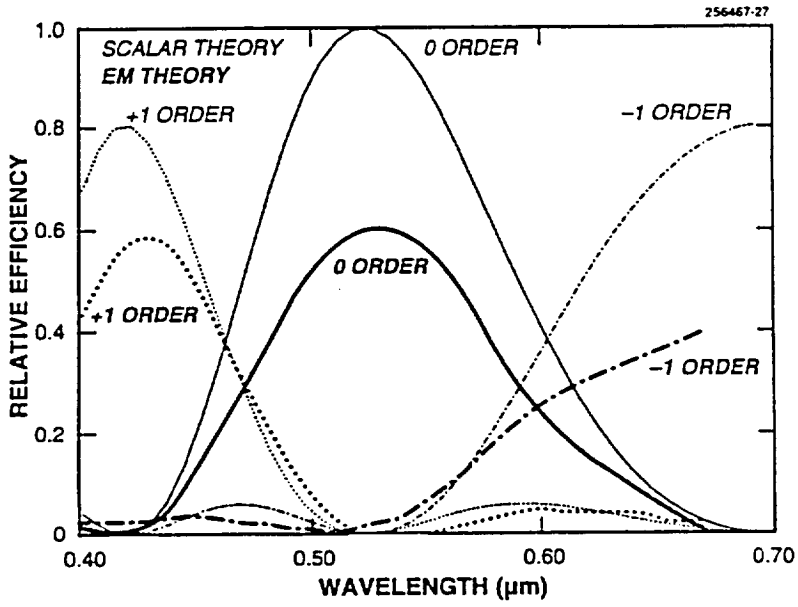

Figure 4-9. Predicted spectral efficiency as function of wavelength for both scalar diffraction theory model and rigorous electromagnetic (EM) calculations. The −1, 0, and +1 order efficiencies are plotted as a function of wavelength.

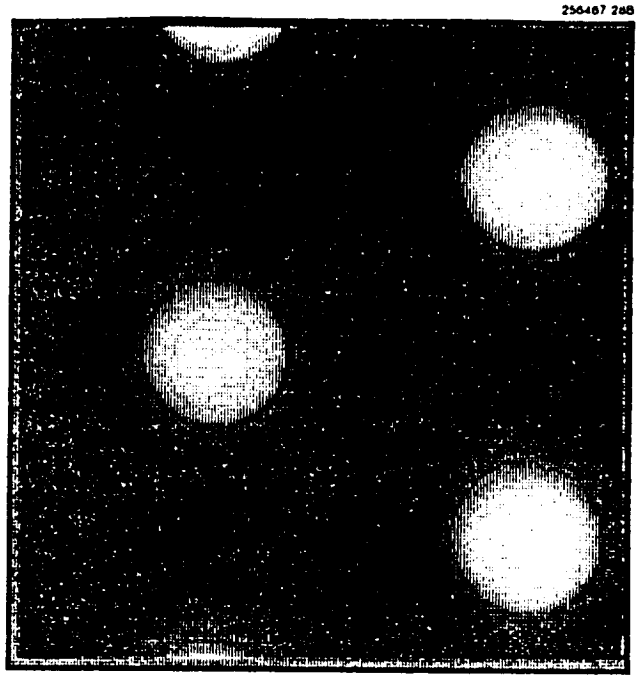

(a)

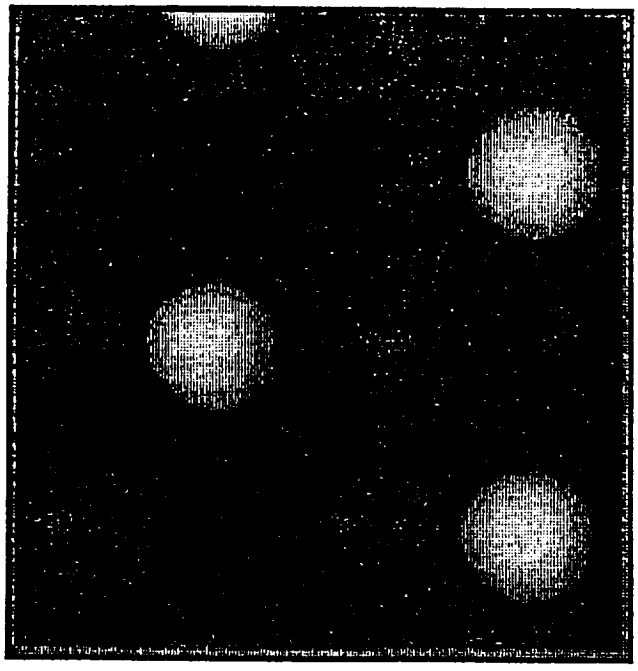

(b)

Figure 4-10. Grating performance showing white light transmitted (a) through microlens array and (b) through color separation grating and microlens array.

the total transmitted light. Scalar theory is considered valid when $T >> \lambda$ and the grating depth is negligible. Because the grating depths for the echelon are not negligible, we expect the 50–60% efficiency predicted by the EM calculations instead of the 80–90% efficiency predicted by the scalar theory. The effects of processing variations on grating performance have also been modeled. The simulations indicate that the etch depth errors must be less than 3% of the minimum step height for the device to function well. Variations in etch depth shift the center frequency to shorter wavelengths if the grating is too shallow and to longer wavelengths if the grating is too deep.

Preliminary evaluation of the color separation optic reveals that the central zero order transmits blue-green light with the red diverted into the −1 order and the blue diverted into the +1 order. The grating operation can be observed using a transmission microscope and a microlens array. The microlens array (either 200-μm-diam ~f/2 photoresist lenses or 500-μm-diam f/4 Corning SMILE lenses) placed on top of the grating, which is illuminated from below, collects the dispersed light. Color is analyzed via a series of color filters placed over the light source. Results are shown in Figure 4-10(a) for illuminated lenslets without the grating and in Figure 4-10(b) for illuminated lenslets with the grating. Overall, this grating separated light with 45% efficiency compared to the predicted 60%.

M. B. Stern
G. J. Swanson
J. E. Curtin

REFERENCES

1. M. E. Lin, B. Sverdlov, G. L. Zhou, and H. Morkoç, *Appl. Phys. Lett.* **62**, 3479 (1993).
2. T. D. Moustakas, T. Lei, and R. J. Molnar, *Physica B* **185**, 36 (1993).
3. S. Strite, M. E. Lin, and H. Morkoç, *Thin Solid Films* **231**, 197 (1993).
4. M. J. Paisley, Z. Sitar, J. B. Posthill, and R. F. Davis, *J. Vac. Sci. Technol. A* **7**, 701 (1989).
5. R. J. Molnar, T. Lei, and T. D. Moustakas, *Mater. Res. Soc. Proc.* **281**, 765 (1993).
6. T. D. Moustakas and R. J. Molnar, *Mater. Res. Soc. Proc.* **281**, 753 (1993).
7. M. W. Farn, R. E. Knowlden, M. B. Stern, and W. B. Veldkamp, in *NASA Conference Publication 3227, Conference on Binary Optics*, H. J. Cole and W. C. Pittman, eds. (NASA, Washington, D.C., 1993), p. 409.

9. References

[1] E.H. Stupp, W. Guerinot, P. Janssen, and L. Hoke, "LCD Rear-Projection Television for Consumer Application", SID 93 Digest, 283-286 (1993).

[2] Y. Glueck, E. Ginter, E. Lueder, and T. Kallfass, "Reflective TFT-Addressed LC light-Valve TV Projectors with High light Efficiency", SID 95 Digest, 235-278 (1995).

[3] H. Dammann, "Color Separation Gratings", Appl. Opt. *17*, 2273 (1978).

[4] MIT/LL Technical Progress Reports. M.W. Farn, R.E. Knowlden, M.B. Stern, and W.B. Veldkamp, "Color Separation Gratings", presented at the Conference on Binary Optics, Huntsville, AL 23-25 February, 1993.

[5] MIT/LL Technical Progress Reports.

[6] E. Schnedler, H.V. Wijngaarde, "Ultrahigh-Intensity Short-Arc Long-Life Lamp System", SID 95 Digest, 131-134 (1995).

[7] M.E. Motamedi, W.H. Southwell, R.J. Anderson, W.J. Gunning, and M. Holz, "High Speed Binary Microlens in GaAs", Proc. SPIE 1544, 33-44 (1991)
M.E. Motamedi, R.J. Anderson, R. De La Rosa, W.J. Gunning, R. Hall, and M. Khoshnevisan, "Binary Optics Thin Film Microlens Array", Proc. SPIE 1544, 22-32 (1992).